REPORT 2

FIRST APPLICATION OF THE SUCCESSIVE TRANSFORMATION METHOD

BY

HECTOR R. ROJAS, Ph.D.

National Aeronautics and Space Administration

HOUSTON, TEXAS

nned Spacecraft Center

REPORT 2

FIRST APPLICATION OF THE SUCCESSIVE TRANSFORMATION METHOD

BY

HECTOR R. ROJAS, Ph.D.

Prepared by:

Lockheed Electronics Company

Houston Aerospace Systems Division

Houston, Texas

For

National Aeronautics and Space Administration

Manned Spacecraft Center

Houston, Texas

February 1967

70058

SUMMARY

Report 1 of these studies described a basic method for predicting lunar surface temperatures, using readings recorded by Surveyor I and extrapolating to obtain surface temperatures in other selected areas. The areas selected were those considered as potential Apollo landing sites.

This second report indicates that the temperature isotherms are directly related to the topographical profile of the surface areas they cover.

If, after further observations by Surveyor II, it becomes evident that the "Successive Transformation Method" provides accurate temperature data, this technique would become a valuable tool for charting the profile of any remote surface where manned spacecraft could be landed.

TABLE OF CONTENTS

REPORT 2

FIRST APPLICATION OF THE SUCCESSIVE TRANSFORMATION METHOD

1. INTRODUCTION

The purpose of this research is to select the safest area on the lunar surface for landing a manned spacecraft. It is therefore necessary to obtain precise information about the behavior of the variation of the temperature on the Moon. Such precise information would not be necessary if the concern was for the spacecraft since Surveyor has already shown capabilities to resist extreme conditions of temperatures. High precision is justified however, since human lives are at stake.

Despite the fact that quality instruments have been used for observing the moon, it is very difficult to get precise information about very small temperature variations, because of instrument and resolution limitations. Another difficulty is that some variations are so small that they are easily compounded with experimental errors, especially in the case of accumulation of errors during reduction of observational data. For example, small peculiar variations of temperature can escape detection because of our inability to discriminate their magnitudes from those of the unavoidable experimental errors previously mentioned.

The resolution limitations of earth observations result in a preference for observations made from space. For example, if we consider a given point on the moon, we know that an instrument could not give the same reading for that point if it was moving from the earth to the moon and making readings (for that point) at various distances along the way. When we compare the temperature measured by Surveyor at the area where it landed with the value obtained on earth for the same area, we are in fact looking for the difference between the minimum and maximum resolutions without taking into consideration, as yet, the additional fact that readings were made by different instruments. However, in this last regard, such differences would always be constant when correlating the respective ratios across the lunar surface and, for this reason, they would not interfere with the computations.

2. SUMMARY OF THE METHOD OF PREDICTING TEMPERATURES

Based on the foregoing premises, the value for the surface temperature of the area where Surveyor landed is very useful for making extrapolations to other areas on the Moon. The precise information we desire can therefore be obtained through the method of successive transformations of data in the following way:

Using a comparable nomenclature to that given in Report I of these studies, let:

T_o = Temperature given by Surveyor in the lunar area where it landed.

T_o' = The predicted temperature for a given point considered on the lunar surface. In other words, T_o' would be the temperature given by the craft if it could move across the surface and read the temperature at the point mentioned.

T = The temperature obtained on Earth for the same point.

From the definition in Report I of P_o and P, we have

$P_o = \frac{T_o}{T}$ for the point where the craft landed.

$P = \frac{T'_o}{T}$ for another point considered at the lunar surface.

Since the data furnished by Surveyor corresponds to a very small area, we then follow the recommendations given in Schemes I and II (see Report 1) and observe some points in close proximity to that point which expands our knowledge into a larger area. In other words, we expand the small area a_o of Scheme 2 and Figure 5 (see Appendix) to the larger area represented by the circle a, a', a'' in the same Figure. We next extend this procedure in the close neighborhood of circle a, a', a'' to the circle represented by b, b', b'', and continue in this way according to the needs of the research but without exceeding selenographic coordinates greater than 2° to avoid systematic errors. From this method, we first get the earth-based observational data for all the points mentioned, including the point where Surveyor landed on the moon, and then establish the different relationships T_o'/T when extrapolating from T_o/T.

To reduce the data for these relationships, we must establish the correlations a/a', b/b',..., h/h' as indicated in Report 1, and then establish the new correlations between these points and other points to be studied. Using the point h_x of Figure 5 as an example, we first successively correlate the points a_x, b_x, c_x, etc. before proceeding to transform successively, going from a_o, in order to get the temperature T_o' at h_x. It is interesting to note that the correlations a/a', b/b',..., h/h' define the angular coefficients of a_x, b_x, c_x, etc. between the corresponding a, a'; b, b'; c, c'; etc. In effect, we have the following:

$$\begin{tikzcd}
a = \frac{T_0}{T_a}, \arrow[d] & a' = \frac{T_0}{T_{a'}}, \arrow[dr] & a_x = \frac{T_0}{T_{a_x}}; \arrow[ll, bend right] \arrow[l, bend left] \arrow[dll] \arrow[d] \\
\frac{a_x}{a} = \frac{T_0}{T_{a_x}} \Big/ \frac{T_0}{T_a}, \arrow[d] & & \frac{a_x}{a'} = \frac{T_0}{T_{a_x}} \Big/ \frac{T_0}{T_{a'}}; \arrow[dll] \\
\frac{a_x}{a'} \Big/ \frac{a_x}{a} = \frac{a}{a'};
\end{tikzcd}$$

$$\begin{tikzcd}
b = \frac{T_0}{T_b}, \arrow[d] & b' = \frac{T_0}{T_{b'}}, \arrow[dr] & b_x = \frac{T_0}{T_{b_x}}; \arrow[ll, bend right] \arrow[l, bend left] \arrow[dll] \arrow[d] \\
\frac{b_x}{b} = \frac{T_0}{T_{b_x}} \Big/ \frac{T_0}{T_b}, \arrow[drr] & & \frac{b_x}{b'} = \frac{T_0}{T_{b_x}} \Big/ \frac{T_0}{T_{b'}}; \arrow[d] \\
& & \frac{b_x}{b'} \Big/ \frac{b_x}{b} = \frac{b}{b'};
\end{tikzcd}$$

$$\vdots$$

$$\begin{tikzcd}
h = \frac{T_0}{T_h}, \arrow[d] & h' = \frac{T_0}{T_{h'}}, \arrow[dr] & h_x = \frac{T_0}{T_{h_x}}; \arrow[ll, bend right] \arrow[l, bend left] \arrow[dll] \arrow[d] \\
\frac{h_x}{h} = \frac{T_0}{T_{h_x}} \Big/ \frac{T_0}{T_h}, \arrow[dr] & & \frac{h_x}{h'} = \frac{T_0}{T_{h_x}} \Big/ \frac{T_0}{T_{h'}}; \arrow[dl] \\
& \frac{h_x}{h'} \Big/ \frac{h_x}{h} = \frac{h}{h'} &
\end{tikzcd}$$

For the summation of different points represented by a_x between a and a' in the first circle, by b_x between b and b' in the second circle, and so on, it is more practical to take advantage of the fact that the temperature gradient on the moon would not be great over short distances. For this reason, and respecting the condition "sine qua non" previously cited, we adopted distances of 1° in longitude and in latitude. This permits us to limit the number of points to be integrated between $a \longleftrightarrow a_x$ and $a_x \longleftrightarrow a'$, $b \longleftrightarrow b_x$ and $b_x \longleftrightarrow b'$, etc. The selection of such points should be made, of course, in increments of 1/2, 1/4, 1/8, etc. of half-arcs $\widehat{aa}_x$; $\widehat{a_x a'}$, $\widehat{bb}_x$; $\widehat{b_x , b'}$,...., $\widehat{hh}_x$; $\widehat{h_x h'}$, but, for practical reasons, it is better to choose the common points of the overlappings which are represented by dark points in Figure 5.

By choosing the common points in the overlap, Figure 5 shows that integrations are not made in a good part of the half-arcs $\widehat{hh}_x$, $\widehat{gg}_x$, $\widehat{ff}_x$ and $\widehat{ee}_x$. However, when going from one area to another, the overlappings permit a check on the computations since the dark points, which are common solutions between two areas, are adequate to assure that operations are going smoothly. Because of this fact, we are actually in a better position to choose the corners of squares in Figure 5 for observing the moon. In effect, it is easier to move the telescope from one degree in longitude to another across the lunar surface and then to change one degree in latitude and repeat the observations in the reverse sense.

The graphical representation given in Figure 5 shows that every summation of equation (6) is composed of several correlations as follows:

$$\left.\begin{array}{l}
\frac{T_0}{T_{h_x}} / \frac{(T_0)_h}{T_{h_x}} / \frac{T_0}{T_h} / \frac{(T'_0)_h}{T_h} \Big/ \frac{T_0}{T_{h_x}} / \frac{(T'_0)_h}{T_{h_x}} \Big/ \frac{T_0}{T_{h'}} / \frac{(T'_0)_{h'}}{T_{h'}} = \frac{h}{h'} \sum_{h_x}^{h} h_n \Big/ \frac{h}{h'} \sum_{h'}^{h_x} h_n = \theta \left(\frac{T'_0}{T} \right)_{h_x} \\
\frac{T_0}{T_{g_x}} / \frac{(T'_0)_g}{T_{g_x}} / \frac{T_0}{T_g} / \frac{(T'_0)_g}{T_g} \Big/ \frac{T_0}{T_{g_x}} / \frac{(T'_0)_g}{T_{g_x}} \Big/ \frac{T_0}{T_{g'}} / \frac{(T'_0)_{g'}}{T_{g'}} = \frac{g}{g'} \sum_{g_x}^{g} g_n \Big/ \frac{g}{g'} \sum_{g'}^{g_x} g_n = \eta \left(\frac{T'_0}{T} \right)_{g_x} \\
\frac{T_0}{T_{f_x}} / \frac{(T'_0)_f}{T_{f_x}} / \frac{T_0}{T_f} / \frac{(T'_0)_f}{T_f} \Big/ \frac{T_0}{T_{f_x}} / \frac{(T'_0)_f}{T_{f_x}} \Big/ \frac{T_0}{T_{f'}} / \frac{(T'_0)_f}{T_{f'}} = \frac{f}{f'} \sum_{f_x}^{f} f_n \Big/ \frac{f}{f'} \sum_{f'}^{f_x} f_n = \zeta \left(\frac{T'_0}{T} \right)_{f_x} \\
\frac{T_0}{T_{e_x}} / \frac{(T'_0)_e}{T_{e_x}} / \frac{T_0}{T_e} / \frac{(T'_0)_e}{T_e} \Big/ \frac{T_0}{T_{e_x}} / \frac{(T'_0)_e}{T_{e_x}} \Big/ \frac{T_0}{T_{e'}} / \frac{(T'_0)_{e'}}{T_{e'}} = \frac{e}{e'} \sum_{e_x}^{e} e_n \Big/ \frac{e}{e'} \sum_{e'}^{e_x} e_n = \varepsilon \left(\frac{T'_0}{T} \right)_{e_x} \\
\frac{T_0}{T_{d_x}} / \frac{(T'_0)_d}{T_{d_x}} / \frac{T_0}{T_d} / \frac{(T'_0)_d}{T_d} \Big/ \frac{T_0}{T_{d_x}} / \frac{(T'_0)_d}{T_{d_x}} \Big/ \frac{T_0}{T_{d'}} / \frac{(T'_0)_{d'}}{T_{d'}} = \frac{d}{d'} \sum_{d_x}^{d} d_n \Big/ \frac{d}{d'} \sum_{d'}^{d_x} d_n = \delta \left(\frac{T'_0}{T} \right)_{d_x} \\
\frac{T_0}{T_{c_x}} / \frac{(T'_0)_c}{T_{c_x}} / \frac{T_0}{T_c} / \frac{(T'_0)_c}{T_c} \Big/ \frac{T_0}{T_{c_x}} / \frac{(T'_0)_c}{T_{c_x}} \Big/ \frac{T_0}{T_{c'}} / \frac{(T'_0)_{c'}}{T_{c'}} = \frac{c}{c'} \sum_{c_x}^{c} c_n \Big/ \frac{c}{c'} \sum_{c'}^{c_x} c_n = \gamma \left(\frac{T'_0}{T} \right)_{c_x} \\
\frac{T_0}{T_{b_x}} / \frac{(T'_0)_b}{T_{b_x}} / \frac{T_0}{T_b} / \frac{(T'_0)_b}{T_b} \Big/ \frac{T_0}{T_{b_x}} / \frac{(T'_0)_b}{T_{b_x}} \Big/ \frac{T_0}{T_{b'}} / \frac{(T'_0)_{b'}}{T_{b'}} = \frac{b}{b'} \sum_{b_x}^{b} b_n \Big/ \frac{b}{b'} \sum_{b'}^{b_x} b_n = \beta \left(\frac{T'_0}{T} \right)_{b_x} \\
\frac{T_0}{T_{a_x}} / \frac{(T'_0)_a}{T_{a_x}} / \frac{T_0}{T_a} / \frac{(T'_0)_a}{T_a} \Big/ \frac{T_0}{T_{a_x}} / \frac{(T'_0)_a}{T_{a_x}} \Big/ \frac{T_0}{T_{a'}} / \frac{(T'_0)_{a'}}{T_{a'}} = \frac{a}{a'} \sum_{a_x}^{a} a_n \Big/ \frac{a}{a'} \sum_{a'}^{a_x} a_n = \alpha \left(\frac{T'_0}{T} \right)_{a_x}
\end{array}\right\} \quad (9)$$

Each of the parts of Equation (9) represent the quantity of radiation emitted in the sector considered. Accordingly, their correlation yields the total amount of such radiation between the reference and the most distant points. As will be shown, the variation of the radiation is a function of the lunar morphology and, for this reason, we must critically analyze the results of the different successive transformations due to different lunar features in a given sector.

To avoid confusion with the transformation coefficient η corresponding to the 7th circle, let η_T equal the summation of the successive transformations coefficients α, β, ..., θ for the temperature. Using the procedure shown on the five examples in Report 1, extrapolate from a_o to h_x by successively transforming in the following way:

$$
\begin{aligned}
&\{[\tfrac{a_0}{a}/\tfrac{a_0}{a'}/\tfrac{a_0}{a}/\tfrac{a_0}{a_x}/\tfrac{a_0}{a}/\tfrac{a_x}{a'}/\tfrac{a_0}{a}/\tfrac{a}{a'}]/[\tfrac{a}{a'}\sum_{a_x}^{a}a_n/\tfrac{a}{a'}\sum_{a'}^{a_x}a_n]+[\tfrac{a_0}{a}/\tfrac{a_0}{a'}/\tfrac{a_0}{a}/\tfrac{a_0}{a_x}/\tfrac{a_0}{a}/\tfrac{a_x}{a'}/\tfrac{a_0}{a}/\tfrac{a}{a'}]/\\
&/[\tfrac{b}{b'}\sum_{b_x}^{b}b_n/\tfrac{b}{b'}\sum_{b'}^{b_x}b_n]+[\tfrac{a}{a'}\sum_{a_x}^{a}a_n/\tfrac{a}{a'}\sum_{a'}^{a_x}a_n]/[\tfrac{b}{b'}\sum_{b_x}^{b}b_n/\tfrac{b}{b'}\sum_{b'}^{b_x}b_n]\}+\{[\tfrac{a_0}{a}/\tfrac{a_0}{a'}/\tfrac{a_0}{a}/\tfrac{a_0}{a_x}/\tfrac{a_0}{a}/\tfrac{a_x}{a'}/\tfrac{a_0}{a}/\tfrac{a}{a'}]/\\
&/[\tfrac{c}{c'}\sum_{c_x}^{c}c_n/\tfrac{c}{c'}\sum_{c'}^{c_x}c_n]+[\tfrac{b}{b'}\sum_{b_x}^{b}b_n/\tfrac{b}{b'}\sum_{b'}^{b_x}b_n/\tfrac{a}{a'}\sum_{a_x}^{a}a_n/\tfrac{a}{a'}\sum_{a'}^{a_x}a_n]/[\tfrac{b}{b'}\sum_{b_x}^{b}b_n/\tfrac{b}{b'}\sum_{b'}^{b_x}b_n/\tfrac{c}{c'}\sum_{c_x}^{c}c_n/\tfrac{c}{c'}\sum_{c'}^{c_x}c_n]\}+\\
&+\{[\tfrac{a_0}{a}/\tfrac{a_0}{a'}/\tfrac{a_0}{a}/\tfrac{a_0}{a_x}/\tfrac{a_0}{a}/\tfrac{a_x}{a'}/\tfrac{a_0}{a}/\tfrac{a}{a'}]/[\tfrac{d}{d'}\sum_{d_x}^{d}d_n/\tfrac{d}{d'}\sum_{d'}^{d_x}d_n]+[\tfrac{c}{c'}\sum_{c_x}^{c}c_n/\tfrac{c}{c'}\sum_{c'}^{c_x}c_n]/[\tfrac{b}{b'}\sum_{b_x}^{b}b_n/\tfrac{b}{b'}\sum_{b'}^{b_x}b_n]/\\
&/[\tfrac{c}{c'}\sum_{c_x}^{c}c_n/\tfrac{c}{c'}\sum_{c'}^{c_x}c_n/\tfrac{e}{e'}\sum_{e_x}^{e}e_n/\tfrac{e}{e'}\sum_{e'}^{e_x}e_n]\}+\{[\tfrac{a_0}{a}/\tfrac{a_0}{a'}/\tfrac{a_0}{a}/\tfrac{a_0}{a_x}/\tfrac{a_0}{a}/\tfrac{a_x}{a'}/\tfrac{a_0}{a}/\tfrac{a}{a'}]/[\tfrac{e}{e'}\sum_{e_x}^{e}e_n/\tfrac{e}{e'}\sum_{e'}^{e_x}e_n]+\\
&+[\tfrac{e}{e'}\sum_{e_x}^{e}e_n/\tfrac{e}{e'}\sum_{e'}^{e_x}e_n/\tfrac{d}{d'}\sum_{d_x}^{d}d_n/\tfrac{d}{d'}\sum_{d'}^{d_x}d_n/\tfrac{e}{e'}\sum_{e_x}^{e}e_n/\tfrac{e}{e'}\sum_{e'}^{e_x}e_n/\tfrac{f}{f'}\sum_{f_x}^{f}f_n/\tfrac{f}{f'}\sum_{f'}^{f_x}f_n]\}+\{[\tfrac{a_0}{a}/\tfrac{a_0}{a'}/\tfrac{a_0}{a}/\tfrac{a_0}{a_x}/\tfrac{a_0}{a}/\tfrac{a_x}{a'}/\tfrac{a_0}{a}/\tfrac{a}{a'}]/\\
&/[\tfrac{f}{f'}\sum_{f}^{f}f_n/\tfrac{f}{f'}\sum_{f'}^{f_x}f_n]+[\tfrac{f}{f'}\sum_{f_x}^{f}f_n/\tfrac{f}{f'}\sum_{f'}^{f_x}f_n]/[\tfrac{d}{d'}\sum_{d'}^{d}d_n/\tfrac{d}{d'}\sum_{d'}^{d_x}d_n]/[\tfrac{f}{f'}\sum_{f_x}^{f}f_n/\tfrac{f}{f'}\sum_{f'}^{f_x}f_n/\tfrac{g}{g'}\sum_{g_x}^{g}g_n/\tfrac{g}{g'}\sum_{g'}^{g_x}g_n]\}+\\
&+\{[\tfrac{a_0}{a}/\tfrac{a_0}{a'}/\tfrac{a_0}{a}/\tfrac{a_0}{a_x}/\tfrac{a_0}{a}/\tfrac{a_x}{a'}/\tfrac{a_0}{a}/\tfrac{a_0}{a'}]/[\tfrac{g}{g'}\sum_{g_x}^{g}g_n/\tfrac{g}{g'}\sum_{g'}^{g_x}g_n]+[\tfrac{g}{g'}\sum_{g_x}^{g}g_n/\tfrac{g}{g'}\sum_{g'}^{g_x}g_n]/[\tfrac{f}{f'}\sum_{f_x}^{f}f_n/\tfrac{f}{f'}\sum_{f'}^{f_x}f_n]/[\tfrac{g}{g'}\sum_{g_x}^{g}g_n/\tfrac{g}{g'}\sum_{g'}^{g_x}g_n/\\
&/[\tfrac{h}{h'}\sum_{h_x}^{h}h_n/\tfrac{h}{h'}\sum_{h'}^{h_x}h_n]\}=P_0+\eta_T P=\frac{T_0}{T}+\eta_T\frac{(T'_0)_h}{T_{h_x}}
\end{aligned}
\tag{10}
$$

In conclusion, if N_T is the number of successive transformations necessary to obtain the transformation coefficient η_T, then:

$$(T'_o)_{h_x} = T_o + (\eta_T)_{h_x} \cdot (T)_{h_x} + \frac{(N)_{hx}}{100}$$

We see that the infinitesimal analysis involved in the successive transformations gives us an opportunity, concerning the behavior of the variation of the temperature, of getting information about the lunar topography with high fidelity. For this reason, such analysis helps us detect small surface variations as will be shown later. However, we already have a graphical representation with the point e_x in Figure 5, where the final results of this analysis show small details on that point which are impossible to detect from earth, even with powerful instruments.

By this means, one can discriminate between the temperatures of points situated in the neighborhood of e_x, because in this example, point e_x is located in a flat area too small to be resolved, and is surrounded by ridges, mountains and craters. Therefore, from this analysis, it appears that e_x is the top of a very small elevation, forming part of a small mountainous region containing numerous small craters. Since temperatures are different for depressions, ridges, mountains and craters, the temperature at e_x is merely an inflection point of those temperatures corresponding to the different topographies situated in its neighborhood. For this reason, when we successively transform observational temperature data from one point to another with respect to the site of Surveyor, we also obtain precise information about the lunar topography previously mentioned.

Because of the inability of instruments to resolve small details such as point e_x of Figure 5, the correlations of equation (9) appears to be the best way to discern the small variations of temperatures which result from small-scale topographic variations of the lunar surface. For example, if the successive transformations of data is applied to a relatively flat surface, the temperature contours would be indicated by straight lines since the radiation coming from a relatively flat surface is uniform.

Such lines change their shape rapidly however, and have the tendency to converge as one approaches the mountains. They form circles in the case of significant craters, but the increments of temperature fluctuate from small to larger values and vice versa when small elevations, depressions or craters are in the area where the successive transformations are applied. Therefore, when the predicted temperature contours are made in the entire sequence of variation, i.e., 0.000, 0.005, 0.010, 0.015, 0.020, 0.025, 0.030, etc. instead of 0.00, 0.01, 0.02, 0.03 etc., one is able to determine a lunar topography variation that is not indicated on the lunar map. A more complete discussion of these results and their implications are included in this document.

3. DISCUSSION OF THE METHOD OF SUCCESSIVE TRANSFORMATIONS OF TEMPERATURE DATA

The lunar surface suggested in Scheme I (see Report 1) corresponds to the Apollo zone of interest for the moon. Accordingly, a map (Pages A-2 through A-6) is presented with the points corresponding to the different numbers N with respect to the position of Surveyor on the moon. With N = 0 for the longitude of Surveyor serving as a reference, we have taken equal distances of 1° in longitude and in latitude and adopted ±10° as the greatest distance from the craft to avoid the systematic errors previously mentioned. In this way, the Apollo zone of interest (at ±45° in longitude and ±10° in latitude) fits with a Mercator projection, whose corresponding numeration is N = 0, 1, 2, 3, ..., 90, without over emphasizing the differences between the Mercator and orthographic projections. However, a correlation must be established for the number N between both projections if we are to apply the successive transformations of data for points whose latitudes are greater than ±10°. As an example, Scheme V (see Appendix) shows that the number N of the point P would not be

$N = 23$, but $N = 33$; and, in the case of the other point P', $N = 9$ instead of $N = 1$.

Selection of the observational data of Shorthill-Saari* has been made for the extrapolation within the successive transformations because they are the most accurate and complete data available. Shorthill-Saari have been observing the moon for several years using very refined observational and data reduction techniques. The lunar isothermes chart of Shorthill-Saari was then used for selecting the earth-based observational data concerning the temperatures T, for each point considered on the map previously mentioned, and taking into consideration the difference between the subsolar point and the apparent disk center. The scan direction of the radiometer has also been taken into consideration. Such a radiometer was used in their observations of the -2° phase angle of the moon on December 18, 1964. The position of Surveyor was determined according to its selenographical coordinates but in introducing the corrections pertaining to the scan direction and, for a more precise orientation, in following the isothermic contours which correspond to major topographical features such as the craters Kepler, Encke, Reinhold, Copernicus, Eratosthenes and Montes Apenninus.

The selenographic coordinates of Surveyor related from the Priority Range 1 have been used. These are 43° 26' West in longitude and 2° 25' South in latitude. Since such coordinates show small differences with other coordinates given by the Jet Propulsion Laboratory, then the mean of T between 43° 00' ⟷ 43° 50', 42° 00' ⟷ 42° 50', etc. has been adopted in order to compensate for errors which would be committed when reading the

---

*Shorthill-Saari, "Lunar Isotherms," Boeing Scientific Research Laboratories - 1966.

temperatures on the lunar chart of Shorthill-Saari. The same thing has been done concerning the latitudes by adopting the mean of T between -2° 00' → -2° 50', -1° 00' → -1° 50', + 1° 00' → + 1° 50' and so on. In this way, the readings of temperatures were first made in longitude and then in latitude for the different points of a given N on the prepared lunar map. The T_o of Surveyor adopted here has been $T_o = 235° \text{ F}$ given by the Jet Propulsion Laboratory in its final report. It must be noted, however, that final report was not at our disposal during the time the successive transformations computations were performed and the value of temperature mentioned was taken from comments about JPL final report by the National Geographic Magazine of September, 1966. An eventual error of the value given has not been taken into consideration. Using the method of successive transformations, we obtain the increment of temperature (δT_o), with respect to the initial T_o, that Surveyor would have registered on the moon if the craft had moved across the lunar surface. In other words, if the initial $T_o = 235° \text{ F}$, E is the error and δT_o is the increment of temperature corresponding to a point other than that of Surveyor, then we have:

$$T_o' = (235° \text{ F} \pm E) \pm \delta T_o$$

From this equation, we see in effect, that δT_o is really independent of E, whatever the value of the error committed by either the sensors of the craft in measuring the temperature of the site where it landed or by JPL when reducing data transmitted to the earth by Surveyor. For reasons which will be explained later, δT_o is always positive when referring to the latitudes. In other words, the sign "$\pm$" for δT_o in the equation above refers to the longitudes with respect to the subsolar point and, for this reason, it is "+" when going to the West and "-" when going to the East.

Following Scheme I of Report 1, the extrapolations of data with respect to the T_o of Surveyor were made from area to area. To facilitate the extrapolations, each area was analyzed for points with latitudes greater than Surveyor and then for points with lesser latitudes. With the exception of the latitude serving as a reference, the axis of Surveyor's point was defined in order to apply equations (9) and the corresponding extrapolations indicated by equation (10). The point of Surveyor is defined as follows:

$$a_o = b_o = c_o = \frac{T_o}{T_{a_o,\ b_o,\ c_o}} = \frac{235^\circ\ F}{232.95^\circ\ F} = 1.008$$

For the area A, the axis of Surveyor's point is as follows:

$$j = \frac{235}{236.12} = 0.995;\quad j' = \frac{235}{214.5} = 1.095;\quad j'' = \frac{235}{232.9} = 1.009$$

$$i = \frac{235}{238.46} = 0.985;\quad i' = \frac{235}{202.04} = 1.163;\quad i'' = \frac{235}{232.67} = 1.010$$

$$h = \frac{235}{239.54} = 0.981;\quad h' = \frac{235}{245.12} = 0.958;\quad h'' = \frac{235}{233.83} = 1.005$$

$$g = \frac{235}{239.54} = 0.981;\quad g' = \frac{235}{245.12} = 0.958;\quad g'' = \frac{235}{233.83} = 1.005$$

$$f = \frac{235}{238.46} = 0.985;\quad f' = \frac{235}{244.04} = 0.960;\quad f'' = \frac{235}{234.95} = 1.000$$

$$e = \frac{235}{234.95} = 1.000;\quad e' = \frac{235}{242.96} = 0.967;\quad e'' = \frac{235}{234.95} = 1.000$$

$$d = \frac{235}{238.46} = 0.985;\quad d' = \frac{235}{240.62} = 0.976;\quad d'' = \frac{235}{236.18} = 0.995$$

$$c = \frac{235}{238.46} = 0.985;\quad c' = \frac{235}{240.62} = 0.976;\quad c'' = \frac{235}{238.7} = 0.985$$

$$b = \frac{235}{237.29} = 0.990;\quad b' = \frac{235}{238.46} = 0.985;\quad b'' = \frac{235}{236.18} = 0.995$$

$$a = \frac{235}{237.29} = 0.990;\quad a' = \frac{235}{236.12} = 0.995;\quad a'' = \frac{235}{236.18} = 0.995$$

For all of the other areas, of course, the axis corresponding to the longitude serving as reference remains the same since they belong to N = 0 and only, for the latitude of Surveyor, their $(a'', b'', c'',\dots, j'')_B$, $(a'', b'', c'',\dots, j'')_C$, etc. vary according to their corresponding values of T read on the lunar isotherms chart.

For this second report, computations have been made from 43° 26' W (N = 0) to 0° 25' W (N = 43). The reason for this is to have at least half of the Apollo zone ready prior to receiving photographs from the second Orbiter. In this way, the identification, in this research, of some of the peculiarities found for the lunar surface can be accomplished as previously stated and the study will be completed at a later time for the whole zone of the Apollo program. The analysis, at the present time, is limited to the 924 points corresponding to the range $0 < N < 43$ in longitude and $-10° < \eta < 10°$ in latitude in increments of one degree in both dimensions.

To provide an example of results obtained, and of the method used, extrapolations are presented in Table 2 (see Appendix) for the Area A of Scheme I and the overlaps with the adjoining Area B. The first column contains the T of Shorthill-Saari and their equivalence in degrees contigrade and fahrenheit. This is followed by the ratios $(j, j'; i, i';\dots; a, a')_A$ and $(a'', a'; b'', b';\dots; j'', j')_A$. The next column contains the $(j_n, j_n = j, j', j'')_A$, etc., corresponding to successive transformations from $(n_{j_x}, n_{i_x}, \dots, n_{a_x})_A$ toward $(j, i, \dots, a)_A$ and toward $(j', i',\dots, a')_A$ as indicated in Figure 5 for latitudes greater than that of Surveyor. As is also indicated in the same figure, columns $(j_x, i_x,\dots,a_x)_A$ and $(j''_x, i''_x,\dots, a''_x)_A$ of Table 2 (see Appendix) contains the correlations given by equation (9). The next column gives the successive transformations contained in equation (10) from a_o to the point under consideration, followed by another column giving the corresponding transformations coefficients η_T which were obtained. The notation T_o' is represented in Table 2 by the column containing the $(T_{j_x}, T_{i_x}, \ldots, T_{a_x})_A$, etc. in order to recall the points which were considered. Finally, for reasons to be later explained, a comparison is shown of the percent difference between the T of Shorthill-Saari and the T_o' obtained by the successive transformation of data with respect to Surveyor.

4. ANALYSIS OF TEMPERATURES OBTAINED FROM THE SUCCESSIVE TRANSFORMATIONS

Temperature differences, which are given in percent in Table 2, may be better understood by analyzing the difference between the successive transformation method and earth-based observations. Briefly, the procedure is as follows:

a. Earth-based observational data have been considered for each of 924 points used in this study

b. Only one temperature has been given by Surveyor for predicting temperatures in other points of the moon

c. Using the method of prediction, the extrapolations have been made by comparing successively the Surveyor temperature (T_o) with each of the earth-based temperatures (T) measured for 924 points

d. Correlations were established among different T_o/T to obtain the δT_o which would be registered by Surveyor at any other site with respect to the site where is landed.

When these conditions are understood, the causal relations of varying temperature for the different points on the moon may be postulated in relation to the lunar topography.

These are:

a. The observational data provides information about the lunar topography (e.g., mountainous regions have higher temperatures than lowlands)

b. Since the correlations of different T_o/T use one measurement read at the lunar surface, the successive transformations of T_o/T from one point to another resolves the difference in temperature that we would not be able to detect from earth

c. In other words, as indicated during the discussion on Figure 5, both methods closely agree on major topographic features, but the successive transformations give more information for small variations in topography.

For this reason, the δT_o obtained by Surveyor is, in fact, the temperature contribution of each point according to its own topographic identity. Accordingly, the quantity $T_o' = T_o + \delta T_o$, defined as "predicted temperature," is the EFFECTIVE TEMPERATURE of a given site as a function of its morphology without taking into consideration the effect of the total temperature of the lunar body over that point. In other words, in this study it appears that we must define temperatures for the moon in the following way:

a. EFFECTIVE TEMPERATURE $T_o' = T_o + \delta T_o$, or "predicted temperature," which is the temperature contribution of the point considered and whose value is obtained with respect to the value measured by Surveyor in the site where it landed

b. RELATIVE TEMPERATURE, or the temperature that usually is considered, is the temperature of a site observed and is affected by the total temperature of the lunar body over a stipulated point.

With these definitions, a discussion of the results with respect to the earth-based observations can be accomplished in the following way:

Let:

$\delta(T_o)_{N,\eta}$ = The temperature increment corresponding to a given number N where η is the transformation coefficient pertaining to the point considered.

$\delta(T_o)_{N,\eta_o}$ = The same as above but referenced to the point situated in the latitude of Surveyor (i.e., where the transformation coefficient is η_o).

$\delta(T_o)(N,\eta)_{Surveyor}$ = The temperature increment in the longitude of Surveyor (N = 0) where $\eta_{Surveyor}$ is the transformation coefficient of the point situated at the same latitude whose transformation coefficient is η.

$\frac{N\ (N-10)}{10\,\eta}$ = The ratio between the number N of successive transformations and its corresponding transformation coefficient, but corrected by a factor of 10 because of the length of 10° used for each area in Scheme 1.

ω = Correction factor relative to the $\delta(T_o)_{N,\eta}$ and $(\delta T_o)(N,\eta)_{Surveyor}$.

T_o' = EFFECTIVE TEMPERATURE (or "predicted temperature") = $T_o + \delta T_o$.

For the latitude of Surveyor then, we have

$$\omega = \left[\frac{N\ (N-10)}{10\eta} \right] \left[\frac{(\delta T_o)^2_{N,\eta_o}}{10^2} \right] \qquad (11)$$

For other latitudes, we have

$$\omega = \left[\frac{N(N-10)}{10\eta} \right] \left\{ \left[\frac{(\delta T_o)_{N,} - (\delta T_o)_{N,\eta_o}}{(\delta T_o)_{N,\eta} + (\delta T_o)_{(N,\eta)\text{Surveyor}}} \right] \Big/ 10 \right\} \qquad (12)$$

Therefore, for any point on the lunar surface, when related to the EFFECTIVE TEMPERATURE given by Surveyor, the relative temperature is:

$$T_{\text{RELATIVE}} = T_{\text{EFFECTIVE}} + \omega \qquad (13)$$

It can now be seen that the differences in percent between the earth-based observational temperatures of Shorthill-Saari and the EFFECTIVE TEMPERATURES given by Surveyor, as shown in the last column of Table 2, are in most cases negative. This results from the fact that the second values represent the contribution temperature of different points substracted from the total temperature of the lunar body for each designated point. It will be shown later that EFFECTIVE TEMPERATURES are nearly equal, equal, or greater than the relative temperatures when they are influenced by the radial lines of major craters. Meanwhile, let us consider, in the following example, another area where the difference between both temperatures is great enough to better show their variation.

Tabulated Data Showing How Determined Parameters Vary With Latitude Along the Longitude 3° 26' West.

<table>
<tr><th colspan="14">AREA D</th></tr>
<tr><th colspan="7">N = 40 ;</th><th colspan="7">$(\delta T_0)_{N,\eta_0} = 0.40$</th></tr>
<tr><th rowspan="2">Latitude</th><th rowspan="2">η</th><th rowspan="2">(δT_0) for N, η</th><th rowspan="2">ω (°F)</th><th rowspan="2">T RELATIVE (°F)</th><th colspan="2">Differences in % with SHORTHILL-SAARI</th><th rowspan="2">Latitude</th><th rowspan="2">η</th><th rowspan="2">(δT_0) for N, η</th><th rowspan="2">ω (°F)</th><th rowspan="2">T (°F) RELATIVE</th><th colspan="2">Differences in % with SHORTHILL - SAARI</th></tr>
<tr><th>RELATIVE</th><th>EFFECTIVE</th><th>RELATIVE</th><th>EFFECTIVE</th></tr>
<tr><td>7° 25' N</td><td>0.10</td><td>0.50</td><td>19.2</td><td>254.70</td><td>+1.2 %</td><td>-6.6 %</td><td>3° 25' S</td><td>0.01</td><td>0.41</td><td>24.0</td><td>259.41</td><td>+ 3.0 %</td><td>-6.6 %</td></tr>
<tr><td>6° 25' N</td><td>0.09</td><td>0.47</td><td>18.7</td><td>254.17</td><td>+0.9 %</td><td>-6.6 %</td><td>4° 25' S</td><td>0.02</td><td>0.42</td><td>24.0</td><td>259.42</td><td>+ 3.0 %</td><td>-6.6 %</td></tr>
<tr><td>5° 25' N</td><td>0.08</td><td>0.47</td><td>18.0</td><td>253.47</td><td>-1.9 %</td><td>-8.0 %</td><td>5° 25' S</td><td>0.03</td><td>0.43</td><td>18.0</td><td>253.43</td><td>+ 0.7 %</td><td>-6.6 %</td></tr>
<tr><td>4° 25' N</td><td>0.07</td><td>0.47</td><td>20.6</td><td>256.07</td><td>-0.8 %</td><td>-8.0 %</td><td>6° 25' S</td><td>0.04</td><td>0.44</td><td>24.0</td><td>259.44</td><td>+ 3.0 %</td><td>-6.6 %</td></tr>
<tr><td>3° 25' N</td><td>0.06</td><td>0.46</td><td>22.0</td><td>257.46</td><td>+0.5 %</td><td>-8.0 %</td><td>7° 25' S</td><td>0.05</td><td>0.45</td><td>21.6</td><td>257.05</td><td>+ 2.9 %</td><td>-5.8 %</td></tr>
<tr><td>2° 25' N</td><td>0.05</td><td>0.45</td><td>24.0</td><td>259.45</td><td>+0.4 %</td><td>-8.0 %</td><td>8° 25' S</td><td>0.06</td><td>0.46</td><td>22.0</td><td>257.46</td><td>+ 4.1 %</td><td>-4.5 %</td></tr>
<tr><td>1° 25' N</td><td>0.04</td><td>0.44</td><td>24.0</td><td>259.44</td><td>+0.4 %</td><td>-8.0 %</td><td>9° 25' S</td><td>0.07</td><td>0.47</td><td>20.6</td><td>256.07</td><td>+ 3.4 %</td><td>-4.5 %</td></tr>
<tr><td>0° 25' N</td><td>0.03</td><td>0.43</td><td>24.0</td><td>259.43</td><td>+0.4 %</td><td>-8.0 %</td><td>10° 25' S</td><td>0.08</td><td>0.48</td><td>19.5</td><td>254.98</td><td>+ 3.1 %</td><td>-4.5 %</td></tr>
<tr><td>0° 25' S</td><td>0.02</td><td>0.42</td><td>24.0</td><td>259.42</td><td>+0.4 %</td><td>-8.0 %</td><td>11° 25' S</td><td>0.09</td><td>0.47</td><td>16.0</td><td>251.47</td><td>+ 1.6 %</td><td>-4.5 %</td></tr>
<tr><td>1° 25' S</td><td>0.01</td><td>0.41</td><td>24.0</td><td>259.41</td><td>+0.4 %</td><td>-8.0 %</td><td>12° 25' S</td><td>0.10</td><td>0.49</td><td>17.8</td><td>253.29</td><td>+ 1.4 %</td><td>-5.6 %</td></tr>
<tr><td colspan="7" rowspan="2">Data for ω and $T_{RELATIVE}$ for the latitude of SURVEYOR according to equation (11) ⟶</td><th>Latitude</th><th>η_0</th><th>$(\delta T_0)_{\eta_0}$</th><th>ω_0</th><th>T RELATIVE</th><th>% RELATIVE</th><th>% EFFECTIVE</th></tr>
<tr><td>2° 25' S</td><td>0.01</td><td>0.40</td><td>19.2</td><td>254.60</td><td>+ 1.1 %</td><td>-6.6 %</td></tr>
</table>

The comparison between RELATIVE and EFFECTIVE TEMPERATURE differences shows that earth-based observational data identifies with RELATIVE TEMPERATURES. The magnitude of these differences is at most about 5 percent near the subsolar point. However, this magnitude is due only to experimental errors. The behavior variation of both temperatures can be summarized in the following way:

a. RELATIVE TEMPERATURES decrease from the subsolar point toward the limbs and toward the poles

b. EFFECTIVE TEMPERATURES also decrease from the subsolar point toward the limbs but increase toward the poles. For this reason the sign "+" always precedes, in this case, the increment δT_o

c. EFFECTIVE TEMPERATURES are influenced by the radial lines of major craters while RELATIVE TEMPERATURES are not

d. Also, the increments δT_o are larger toward the Southern Pole than toward the Northern Pole while RELATIVE TEMPERATURES do not show such a variation. This behavior of δT_o is due to the fact that more mountains and craters exist in the Southern Hemisphere of the moon than in the Northern Hemisphere.

For graphically analyzing (b), (c), (d), an example is given with EFFECTIVE and earth-based temperatures for latitudes greater than that of Surveyor and corresponding to the Area A of Scheme I. The results from successive transformations are given in Table 3 (see Appendix) where they are added to the transformation coefficients η_T corresponding to the different N considered. Also added are the errors ΔT committed in the successive transformations. Since $N/100 < P_o$, these ΔT have been computed according to the first case of equation (8) in Report 1. Also, because of equations (11) and (12), they have been corrected by the same factor. In other words, for a given longitude corresponding to a given N with respect to N = 0 of the longitude of Surveyor, we have:

$$\Delta T = \left\{ \left[\frac{(T_o)_{N,\eta}}{T_{N,\eta}} + \frac{N}{100} \right] - \frac{(T_o)}{T_{(N,\eta)\text{Surveyor}}} \right\} \left(\eta_N + \eta_{\text{Surveyor}} \right)$$

We can see in Table 3 that the maximum error from point-to-point is $\Delta T = \pm 0.0005$. For a given point with respect to the site where Surveyor landed, ΔT is increasing slowly with N. For the most distant point N = 45 and $\eta = 0.12$, at 7° 25' N in the longitude of the subsolar point, the error accrued in the successive transformations is $\Delta T = 45\ (0.0005) = 0.0225$, which is just a little larger than the maximum error 0.02 mentioned in page 7 of Report 1.

The graphical illustration is given in Figure 6 (see Appendix) where the logarithms were used to reduce the scale for the temperatures. Comparison of these data with the observational curves show that the variation of EFFECTIVE TEMPERATURES is practically uniform. According to Table 2, the rate of this uniform variation is 0.01° F per selenographical coordinate if the radiation comes from a relatively flat surface. With topographical formations, this rate is not modified in its basic value 0.01 but is only affected by a given multiple such as 2(0.01), 2(0.01), etc. The multiple is a function of the type of topography and, for this reason, the EFFECTIVE TEMPERATURE contours have different shapes for small elevations, high mountains, and craters. They have capricious distribution in the case of depressions and fissures.

We can see in Figure 6 that EFFECTIVE TEMPERATURES are greater than earth-based data temperatures at 43° 26' W for the latitudes 2° 25' S; 1° 25' S and 0° 25' S. This is due to small depressions before and after the small mountains located at 1° 25' S of this longitude. These small depressions are not clearly indicated on the lunar map and an Orbiter photograph will be necessary to confirm their existence. At 42° 26' W and 2° 25' S; 40° 26' W and 7° 25' N; 37° 26' W and 5° 25' N; 36° 26' W and 7° 25' N, the EFFECTIVE TEMPERATURES are almost equal to the data obtained from earth. This case of $T_{\text{effective}} \approx T$ is due to the existence of more important depressions near larger mountains. $T_{\text{effective}} = T$ at 43° 26' W and 2° 25' N; 43° 26' W and 7° 25' N; 42° 26' W and 7° 25' N; 41° 26' W and 7° 25' N; 37° 26' W and 6° 25' N;

37° 26' W; and 7° 25' N is due to the existence of craters in flatter lowland regions which lack pronounced rims. Most of these craters are not indicated on the lunar map and only Orbiter photographs could show their presence on the sites mentioned. The case $T_{effective} < T$ results from the influence of mountains and rayed patterns (radial lines) associated with major craters. Both contours have a tendency to run parallel in this case and the discontinuities of such parallelism may be described in the following way:

a. If discontinuities are going down, there is a relatively flat surface in the neighborhood of mountains

b. If they are going up, the relatively flat surface has surrounding relief and the intensity of the discontinuity of earth-based temperature contour is a function of the relief elevation.

The influence of rayed patterns of major craters on the EFFECTIVE TEMPERATURES is indicated on the map showing the portion of Area A which is discussed in this report. To better show the indicated effect, the sense of the differences between T'_o and T is graphically represented instead of T'_o alone. These differences must be arranged in the sequence $T'_o < T$ or $T'_o < T \rightarrow T'_o \approx T \rightarrow T'_o = T$ but never $T'_o > T \longrightarrow T'_o \approx T \rightarrow T'_o = T \rightarrow T'_o < T$. Only a few lines have been drawn on the map, from which we can notice the following facts:

a. Between the radii, and with the exception of the very near regions of major craters, the sense is always $T'_o < T$

b. Close to major craters, it is always $T'_o \approx T$ or $T'_o = T$

c. The $T'_o \approx T$ or $T'_o = T$ have the tendency to distribute along radial lines normal to other radial lines

d. The $T'_o < T$ situated or normal radial lines in the neighborhood of major craters are due to relatively flat surface surrounding higher and lower elevations

e. For radial lines other than those normal to each other, it is easy to recognize the kind of anomalies that occur on lines where the sequence must be $T'_o < T$, at least up to arcs adjoining major craters. These are anomalies $T'_o > T$, $T'_o \approx T$ or $T'_o = T$ of the sequence already cited.

A deeper study of this effect will be made in the third report of this series.

5. USE OF THE SUCCESSIVE TRANSFORMATIONS TEMPERATURE RESULTS FOR SELECTING LANDING SITES

In view of the fact that the EFFECTIVE TEMPERATURES are a function of the lunar morphology, the opportunity has been taken to use them for selecting landing sites. The intention is to do this for the whole lunar zone of the Apollo program but, in this second report, only the latitudes greater than that of Surveyor for Area A are considered. The application of the SECOND STEP suggested in Report 1 is shown in Figure 7 (see Appendix) where η, N, Slope of T_o are plotted according to the data contained in Table 3. In other words, Figure 7 is the graphical application of Figure 1 of Report 2 after translation of the P_o and P into the corresponding ratios T_o/T and T'_o/T mentioned in the beginning of this report. With regard to the sites proposed by NASA, the application of this method is considered easy since the Apollo zone is analyzed for every degree of selenographical coordinates.

In Figure 7, it is shown that the data plotted on or near the slope of T_o corresponds to the following points: 40° 26' W, 1° 25' S; 39° 26' W, 0° 25' S; 38° 26' W, 0° 25' S; 37° 26' W, 0° 25' N; 36° 26' W, 2° 25' N; 35° 26' W, 1° 25' N; 34° 26' W, 3° 25' N and 33° 26' W, 4° 25' N. For latitudes greater than that of Surveyor in Area A, such sites barely separate the two following lunar regions:

a. A region to the South of Surveyor where ridges, rifts and small craters are abundant

b. A region to the North of Surveyor where mountains and pronounced craters are also abundant. The area separating the regions is practically a flat surface broken occasionally by small craters distributed in some sectors of this line of separation.

The expression "good site" was used in Figure 7 to designate the sites with the following selenographical coordinates: 40° 26' W, 1° 25' S; 39° 26' W, 0° 25' S; 38° 26' W, 0° 25' S; 37° 26' W, 0° 25' N; 34° 26' W, 3° 25' N; 33° 26' W, 4° 25' N. In these sites, the relatively flat surface has the same aspect as that of Surveyor's site. The point 36° 26' W, 2° 25' N has been designated as "next best" and it is close to the crater Encke B and relatively high elevations are near the flat surface. Finally, the designation of "last best" for 35° 26' W, 1° 25' N is due to the fact that the site is located close to a ridge.

However, the slope of T_o in Figure 7 indicates only what would be the most convenient site for landing if that portion of Area A is determined to be of interest. In other words, the slope of T_o not only indicates the site having optimum conditions for the spacecraft, but for the human being as well. This means that other good sites can be selected with respect to the one where

Surveyor landed, but not necessarily in the same portion of Area A under consideration. For locating such an optimum site, it is necessary to proceed in the following way:

a. As indicated in Figure 8 (see Appendix) the points on or near of the slope of T_o are placed on the lunar map to determine the arc extension covered by them

b. Since the minimum given by the increment temperature $(\delta T_o)_{Surveyor} = 0.00$ and maximum of the $(\delta T_o)_{P_8} = 0.17$ are the limits of such an arc, then one determines the angle β corresponding to it and whose tangent is equal to unity. The locus point 0 of the arc $\overset{\frown}{P_o P_8}$ is the site we seek, having, with respect to the site of Surveyor, the maximum conditions previously mentioned.

The locus point 0 of the arc $\overset{\frown}{P_o P_8}$ is situated at 46° 55' W and 12° 52' N, between the craters Marius A and C. The relatively flat surface is extensive and appears, then, to be an ideal area for landing. The RELATIVE TEMPERATURE is also lower than that corresponding to the site where Surveyor landed, as will be shown. It is noted that the site of the locus point 0 is almost out of the influence of the radial lines associated with the crater Kepler. If the arc $\overset{\frown}{P_o P_8}$ has not given a locus point completely out of such an effect, it is because of the presence of more abundant medium diameter craters and mountains near the crater Marius C. However, the locus point is protected by the crater Marius A from the temperature effects associated with rayed patterns in that area.

6. EFFECTIVE TEMPERATURES ISOTHERMS OBTAINED FROM THE SUCCESSIVE TRANSFORMATIONS

To better show the capability of the successive transformations method to resolve small variations of the lunar topography, only the increments δT_o are used to draw isotherms in the following way:

a. With the purpose of examining the general shape of contours, a rough isotherm chart was prepared for one half of each area considered on the western region of the Apollo program lunar zone, this half was then combined with the isotherm chart for the area in the smaller latitudes. As an example, one of these drawings is presented in Figure 9 (see Appendix) for latitudes greater than that of Surveyor in Area A; points appearing as anomalous are indicated by A, B, C, D,..., K

b. The two halves of each area were put together in order to join the corresponding isotherms; necessitating a second fit of the drawing

c. Finally, all areas were put together and a third fit was accomplished to obtain the correct isotherms for the cited western region of the Apollo program.

A transparent master was prepared for the final isotherm chart and superimposed over the lunar map presented at the end of this report. For latitudes greater than of Surveyor in Area A, the remaining anomalous points were indicated with ovals; the same method was also used for smaller latitudes. These points are located at the following selenographical coordinates: 6° 25' N at 43° 26' W and 42° 26' W; 41° 26' W, 2° 25' N; 1° 25' S, 42° 26' W; 2° 25' S, 41° 26' W and 43° 26' W, 3° 25' S. No attempt has been made to correct the contours in sites which did not correspond to the shape of lunar features. For instance, these contours do not follow the topography in: 36° 26' W, 4° 25' N (the crater Encke); 36° 26' W, 2° 25' N (the crater Encke B); 40° 26' W, 0° 25' N (the crater Encke E); 36° 26' W, 0° 25' N (the crater Encke C) and so on. The reason for not correcting these contours results from:

a. The desire to do a first analysis of isotherms using only the results given by the successive transformations

b. To use the results obtained from such an analysis to later study the sites mentioned above and, also, to determine the nature of structure and composition with respect to the major features situated in their neighborhood.

A study of the lunar map which contains the superimposed contours of isotherms (see last pages) indicates the following:

a. In the Apollo zone of interest, the contours have the tendency to become parallel approximately every 3° in longitude. At first, it was thought that this was due only to some "mathematical effect" of formulae used in the computations. It was later realized, however, that this pattern is due to the lunar topography itself. In effect, most of the time the lunar map shows distributions of features, such as elevations and craters, along the parallels of these contours. Because of the fact that the lunar zone of the Apollo program is roughly a rectangular surface, then the distribution of contours only appears parallel in this zone at, approximately, an interval of 3° in longitude between each group of such contours. However, when going beyond ±10° in latitude, this distance progressively decreases and, for this reason, all of these contours converge toward the poles. Before and after each group of such contours located in the Apollo zone, the EFFECTIVE TEMPERATURE values are not continuous; when moving North and South, it is found that the sequences 0.11 → 0.11 → 0.11, 0.12 → 0.12 → 0.12, 0.13 → 0.13 → 0.13, 0.14 → 0.14 → 0.14, etc., for example, do not exist but are supplanted by the sequences 0.11 → 0.11 → 0.11, 0.14 → 0.14 → 0.14, 0.17 → 0.17 → 0.17, 0.20 → 0.20 → 0.20, etc. Unfortunately the length of this second report does not permit a deeper study of this peculiar distribution of features across the lunar surface. However, this will be done in the third report.

b. Isotherm contours, corresponding to the latitudes between each of the groups mentioned, are distributed at constant intervals of 0.01° F per degree latitude; only the multiple is modified according to the kind of lunar features encountered. In spite of the length of this report, one can briefly describe the variation of multiples in the following way:

(1) If a relatively flat surface is found, the EFFECTIVE TEMPERATURE contours have the tendency to remain linear in the same latitude and, approximately, between every -3° in longitude. This indicates that the lunar radiation is, in this case, uniformly distributed. Because of this, only a factor of 1 affects the values through the different and the linear tendency remains so long as the lunar topography remains the same

(2) When approaching a mountain, the linear tendency is modified by a factor of 2 and the contours are convergent between the preceding and following values of the EFFECTIVE TEMPERATURES

(3) On a mountain, the linearity completely disappears; the path of a given contour is only affected, in this case, by the path of the other contours which are in its neighborhood

(4) Because of (3), the contours have a tendency to adopt a circular shape in the case of significant craters

(5) The contours diverge in the case of depressions, in the reverse sense as mentioned in (2). The affecting factor is varying in the following manner: 1.(0.01); 1.2.(0.01); 1.2.3.(0.01), etc. according to the importance of depressions

(6) The discontinuity of divergent contours, such as 0.05 → 0.04 → 0.03 → 0.02 → 0.03 → 0.02 → 0.03 → 0.04 → 0.05, is due to the existence of craters without pronounced rims.

c. From the Surveyor location to the subsolar point, and with respect to the latitude of Surveyor, the isotherms display a tendency to adopt the shape of a reversed "C" and are only modified by rayed pattern craters. This reversed "C" shape is clearly seen from Surveyor's longitude until about 27° 26' W, where the radial line effect associated with Copernicus becomes important. It progressively disappears between 27° 26' W and 14° 26' W because the rayed pattern also disappears. Between 14° 26' W and 8° 26' W, the reversed "C" with the region 19° 26' W → 14° 26' W; however, its shape is now affected by the rayed crater situated near Mosting A. Between 8° 26' W and 3° 26' W, such reversed "C" is again seriously modified due to the fact that the influence of the rayed crater near Mosting A is stronger but its shape finally reappears between 3° 26' W and the longitude of the subsolar point. One can also notice that between 19° 26' W and 14° 26' W, the modifications suffered by the reversed "C" are different for greater and smaller latitudes than that of Surveyor. In effect, such modifications are much more pronounced in the upper latitudes because of the rayed pattern of Copernicus. They are slighter in lower latitudes despite the presence of the crater Fra Mauro, because this crater does not have nearly the same pronounced structure as Copernicus.

7. THE SMALL LUNAR FEATURES PREDICTED BY THE SUCCESSIVE TRANSFORMATIONS

The variation behavior of multiples, mentioned in the preceding section, is the characteristic serving to identify differences in the lunar topography. This characteristic is especially useful in identifying the type of small variations discussed when the contours are exceedingly close or, as we have previously seen, when such contours do not follow the shape of a lunar feature as shown on available lunar topographic maps. Where using multiples for such purpose, however, it is convenient to study a restricted sector, especially to study in detail a site which has been selected for landing. It would be less practical to use the variation of multiples to study the large areas such as the western part of the Apollo zone. For this reason, an idea proposed by Mr. Roland R. Vela, of the Mapping Sciences Branch, has been followed and another transparent master prepared to represent graphically the variation behavior of multiples.

This transparent master of Vela has also been superimposed over the lunar map and included in the Appendix of this report. The increments δT_o have been multiplied by a factor of 100 and are given only contours having a basical difference of 5/100. These heavier isotherm lines allow easier separation of values. The drawings corresponding to the cited variation of multiples have also been prepared in such a way that they may be more easily read by people familiar with the topographic contour mapping technique.

In this way, the prompt identification of the small features, not found on the lunar map, but shown by the successive transformations, is facilitated. Preparation of a list of such small features for the half of the Apollo zone of interest considered in this research would require excessive time. As an example, for Area A, in Vela's drawing, the following predictions can be made:

a. There must be a depression with two small craters located approximately at 43° 26' W, 6° 25' N and 42° 26' W, 6° 25' N. These two small craters are without pronounced rims.

b. Starting at about 45° 00' W and ending at 41° 26' W, between 3° 25' N and 4° 25' N, there must be a small ridge that ends abruptly at a feature seen on the lunar map at 41° 26' W, 4° 25' N.

c. Another depression must separate an elevation seen on the lunar map at 40° 26' W, between 1° 25' N and 2° 25' N. The depression is centered at 1° 55' N and a small crater without pronounced rims is indicated.

d. A small elevation must exist at 41° 26' W, 2° 25' N. This small elevation must be an obscured continuation of the less distinct crater rim of Maestlin R4.

e. A small elevation and small crater without pronounced rims must exist at 42° 26' W, 1° 25' S.

f. A small elevation with some small craters without pronounced rims must exist at 41° 26' W, 2° 25' S.

g. A small elevation with some small craters without pronounced rims must exist at 42° 26' W, 3° 25' S.

h. A small elevation near the crater Flamsteed A and with small craters must exist at 42° 26' W, 4° 25' S.

i. Because of the tendency of contours to diverge toward the West, the features identified at a, e, f, g, and h must be accompanied of depressions.

j. A small ridge must be present at 44° 00' W extending to 40° 26' W between 6° 25' S and 7° 25' S. Small craters are indicated along this trend.

k. A small mountain must be the main body of the crater Letrone B since this crater is the locus point of convergent contours between 42° 26' W → 40° 26' W and 10° 00' S → 12° 00' S.

Identification will be made, within the Orbiter Photographs, of the small details given by the successive transformations of the lunar topography. The purpose is to make a more extensive study on this subject from an astronomical point of view.

8. THE PREDICTED LUNAR RELATIVE TEMPERATURES WITH THE SUCCESSIVE TRANSFORMATIONS

Through the preceding explanations, it can be seen that RELATIVE TEMPERATURES are predictable by the successive transformations method. For example, concerning the landing site suggested by η, N, slope of T_o for latitudes greater than that of Surveyor in Area A and with respect to the Surveyor site, we have the following data:

$N = -3.5$ $(\delta T_o)_{N,} = 0.14$ $\eta_o = 0.01$

$\eta = 0.22$ $(\delta T_o)_{N,\eta_o} = -0.03$ $(\delta T_o)_{(N,\eta)_{\text{Surveyor}}} = 0.17$

Since the locus point 0 is at 46° 55' W and 12° 52' N, and out of the rectangular Apollo zone, we must then introduce the correction η/η_o between orthographic and Mercator projections. Also, because the locus point 0 is situated to the West of Surveyor's longitude, equation (12) becomes:

$$W = \frac{(-N)\left[(-N) - 10\right]}{10\eta}\left\{\left[\frac{-(\delta T_o)_{N,} - (\delta T_o)_{N,\eta_o}}{-(\delta T_o)_{N,\eta} - (\delta T_o)_{N,\eta\,\text{Surveyor}}}\right] \cdot \left(\frac{\eta/\eta_o}{10}\right)\right\}$$

Thus, Predicted T_{RELATIVE} = Predicted EFFECTIVE TEMPERATURE

$$T_o' + \omega$$

$$= 235°.14 \text{ F} - 11°.82 \text{ F} \approx 223°.3 \text{ F}$$

$$\approx 92°.1 \text{ C}$$

If we consider now the flight of Surveyor III, scheduled for February 15, 1967, the predicted RELATIVE TEMPERATURE is 263°.48 F, provided the spacecraft lands at 0.67° W and 0° latitude.

The predicted RELATIVE TEMPERATURE becomes 247°.49', however, if the spacecraft is launched February 18 thru 22, and lands at 22°.75 W and 3°.75 S.

Note

The above predictions were made on December 9, 1966. This fact is established in order that the accuracy of the described method may be later assessed.

APPENDIX

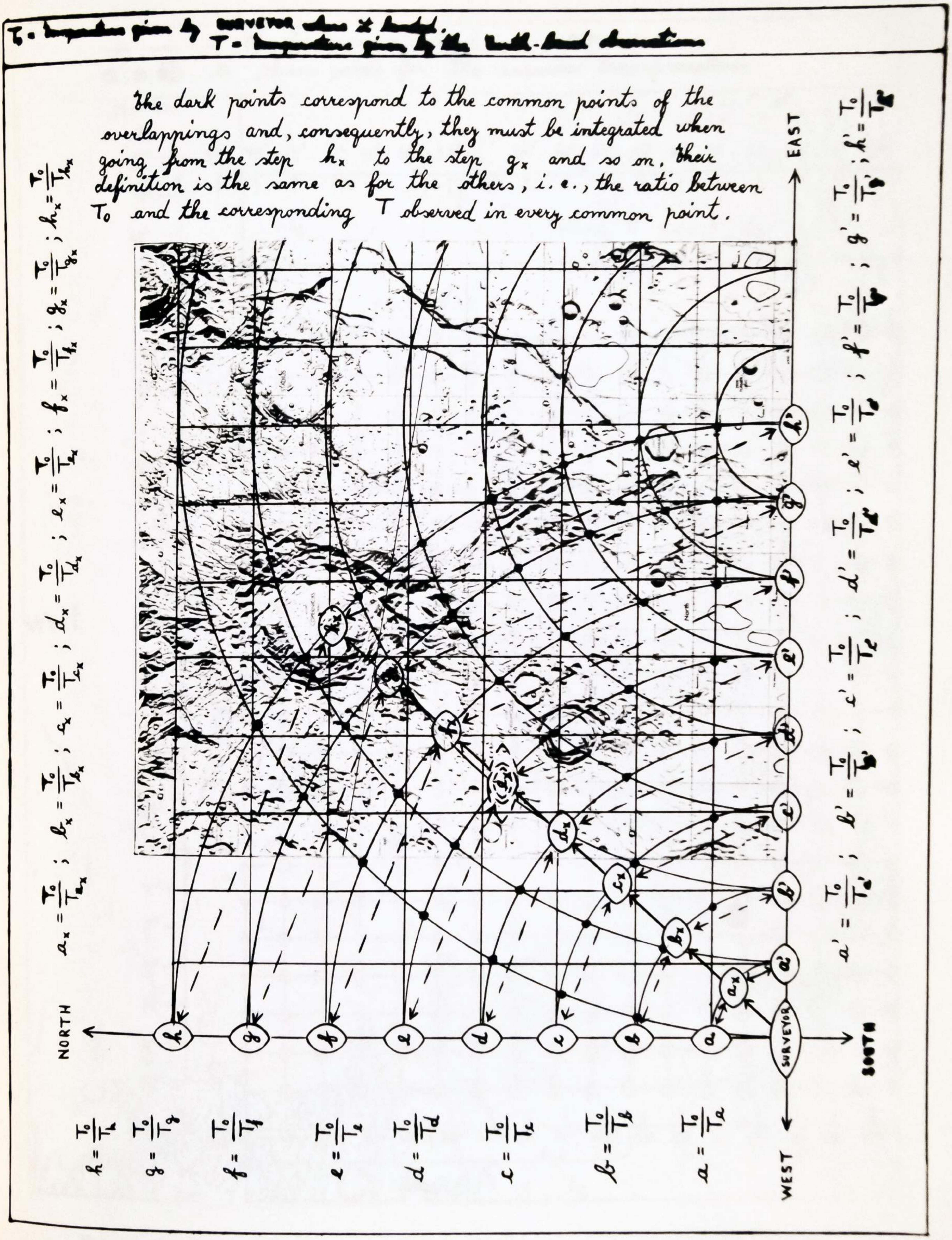

T_0 = temperature given by SURVEYOR when it landed.
T = temperature given by the earth-based observations

The dark points correspond to the common points of the overlappings and, consequently, they must be integrated when going from the step h_x to the step g_x and so on. Their definition is the same as for the others, i.e., the ratio between T_0 and the corresponding T observed in every common point.

Figure 5

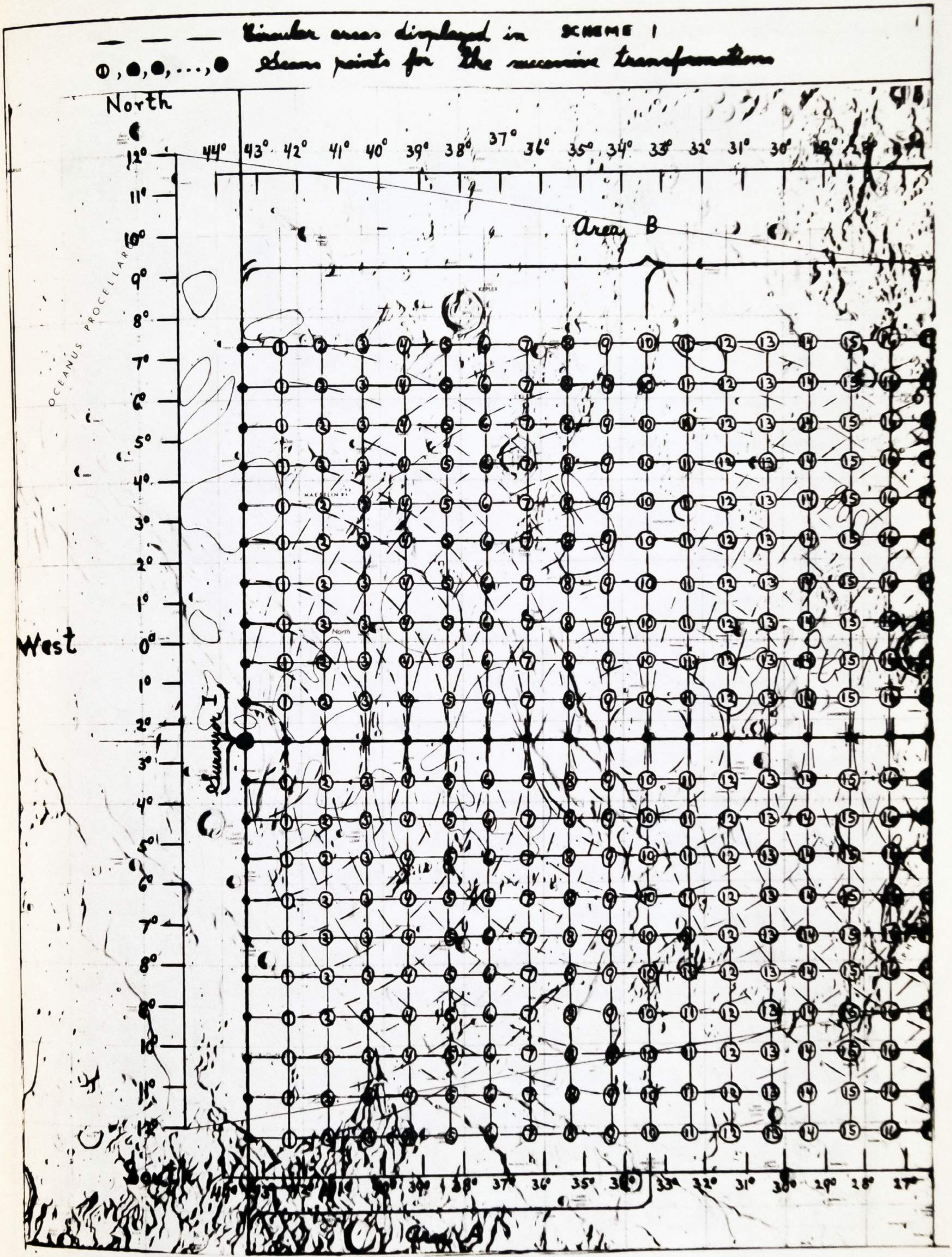

Map of the Moon Containing the Points To be Observed, Whose Data Will Be Reduced by the Successive Transformation Method - Part I

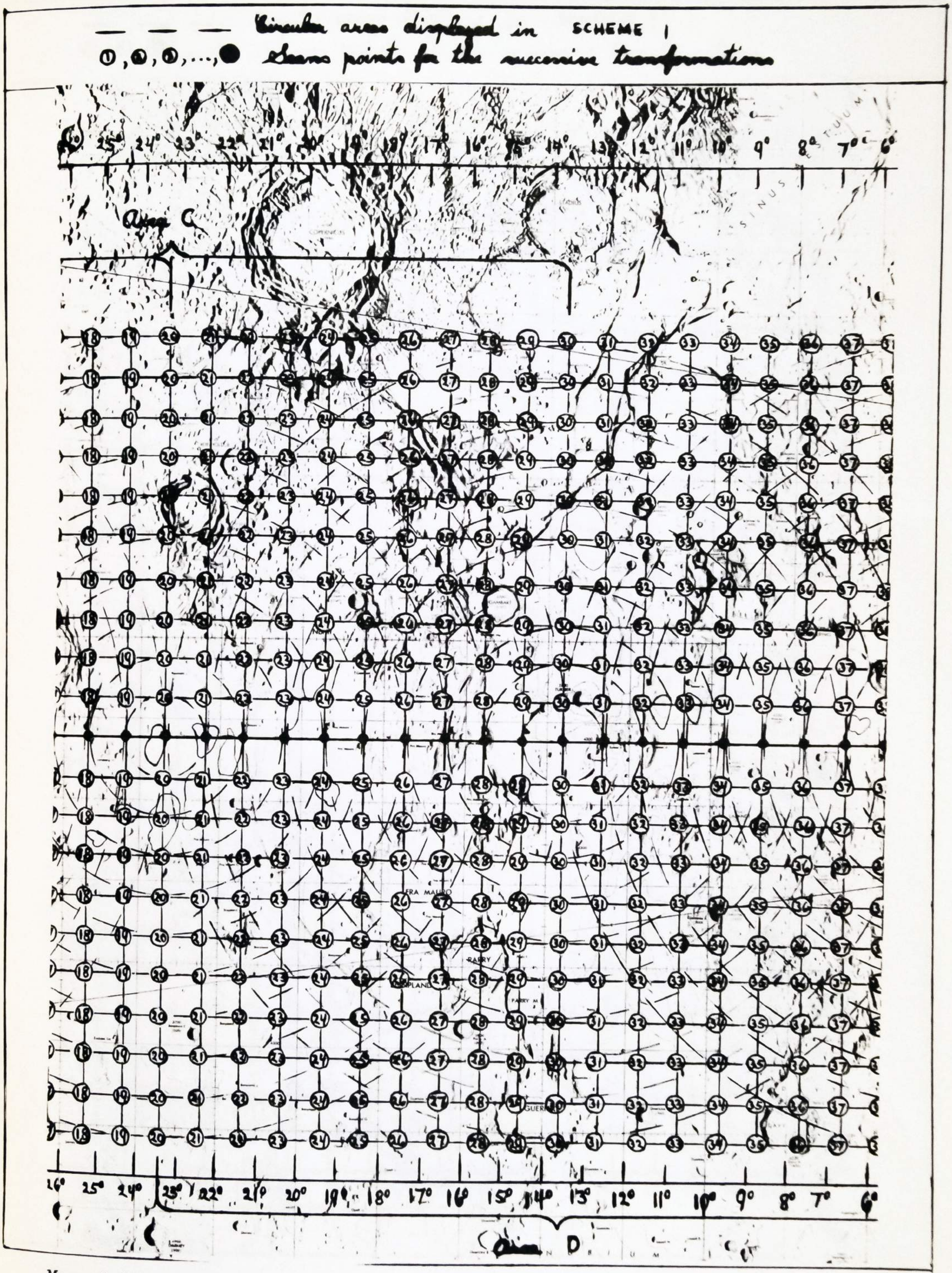

Map of the Moon Containing the Points To Be Observed, Whose Data Will Be Reduced by the Successive Transformation Method - Part II

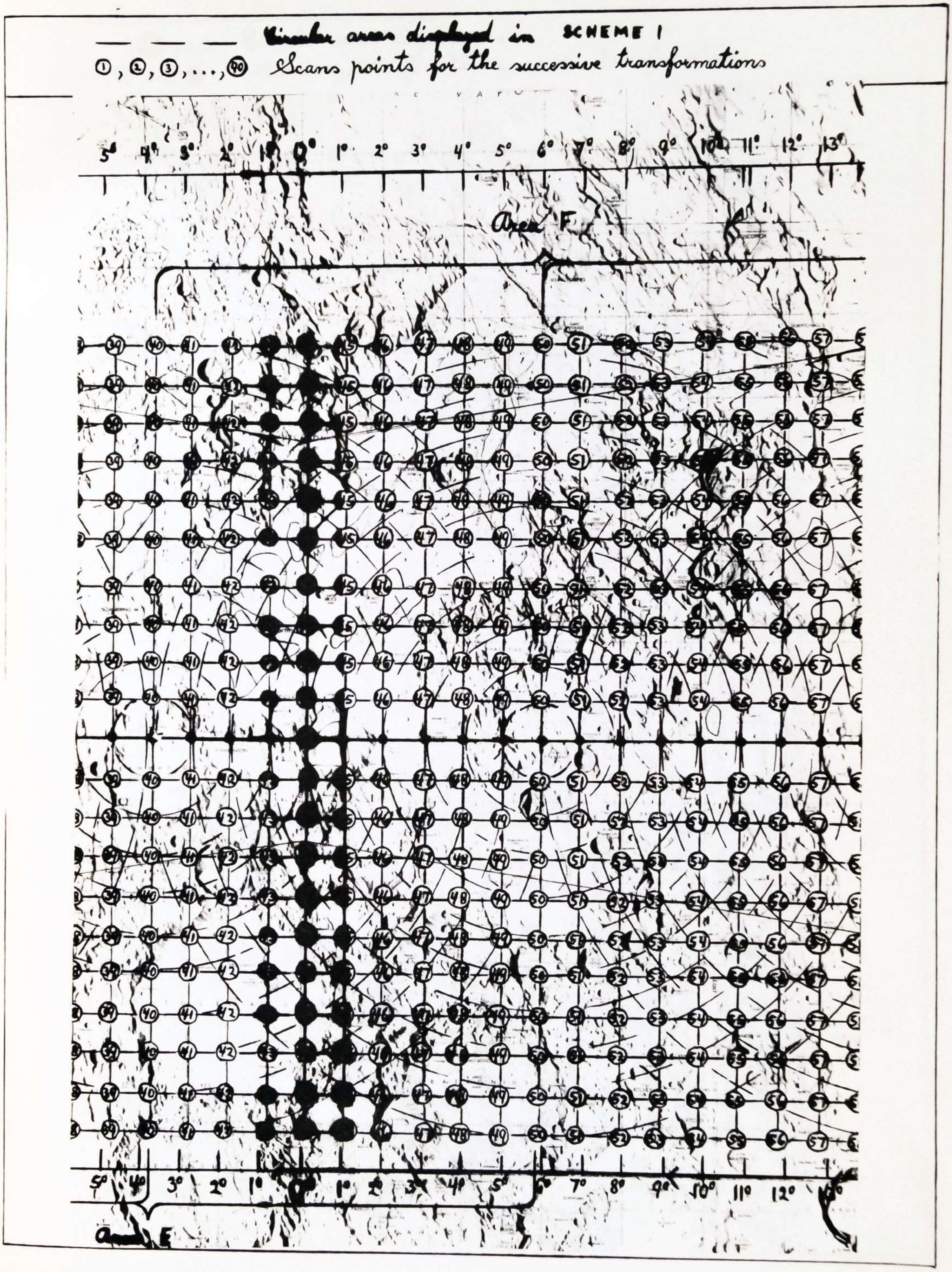

Map of the Moon Containing the Points To Be Observed, Whose Data Will Be Reduced by the Successive Transformation Method - Part III

Circular areas displayed in SCHEME I

①,②,③,...,(90) Scans points for the successive transformations

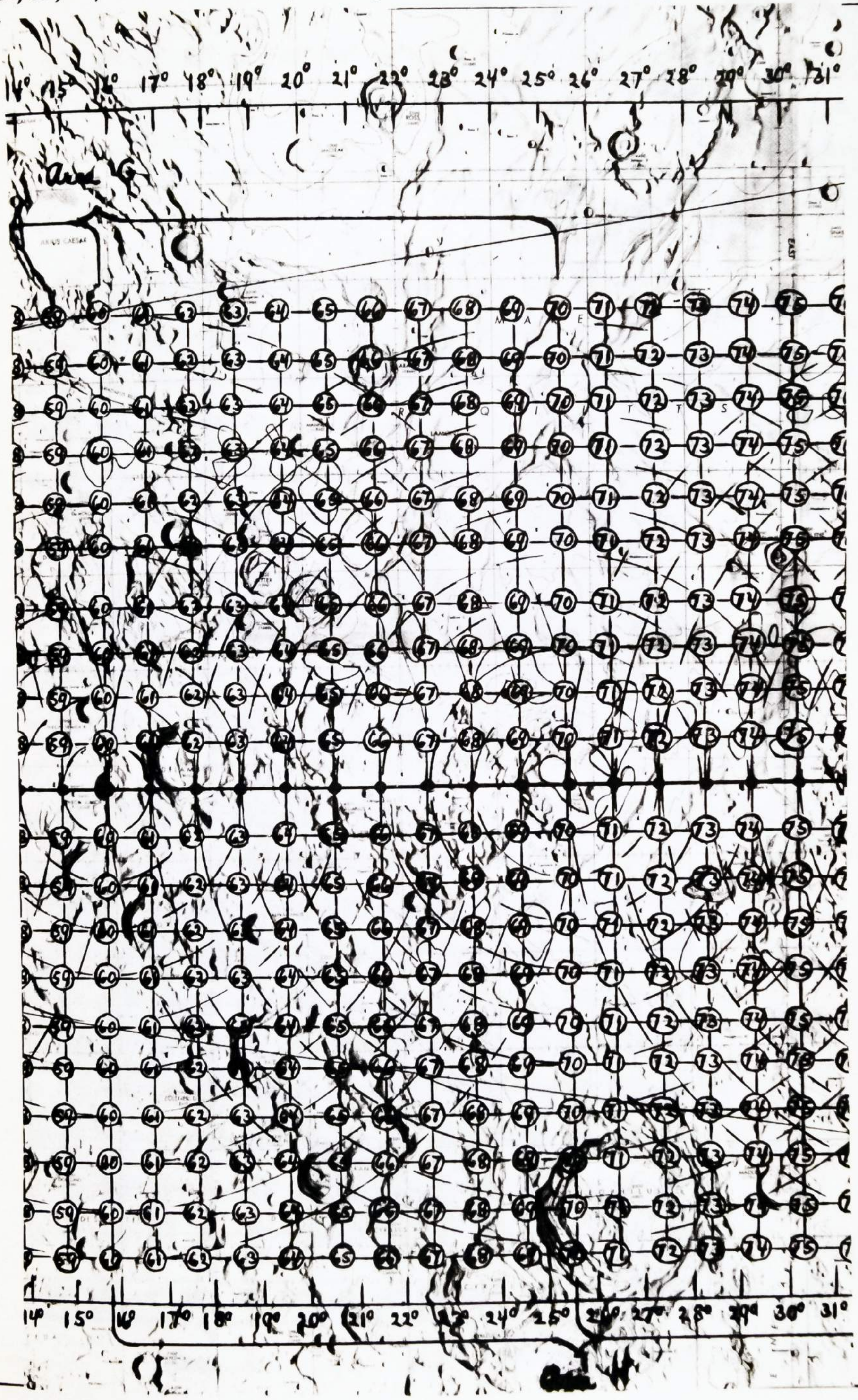

Map of the Moon Containing the Points To Be Observed, Whose Data Will Be Observed by the Successive Transformation Method - Part IV

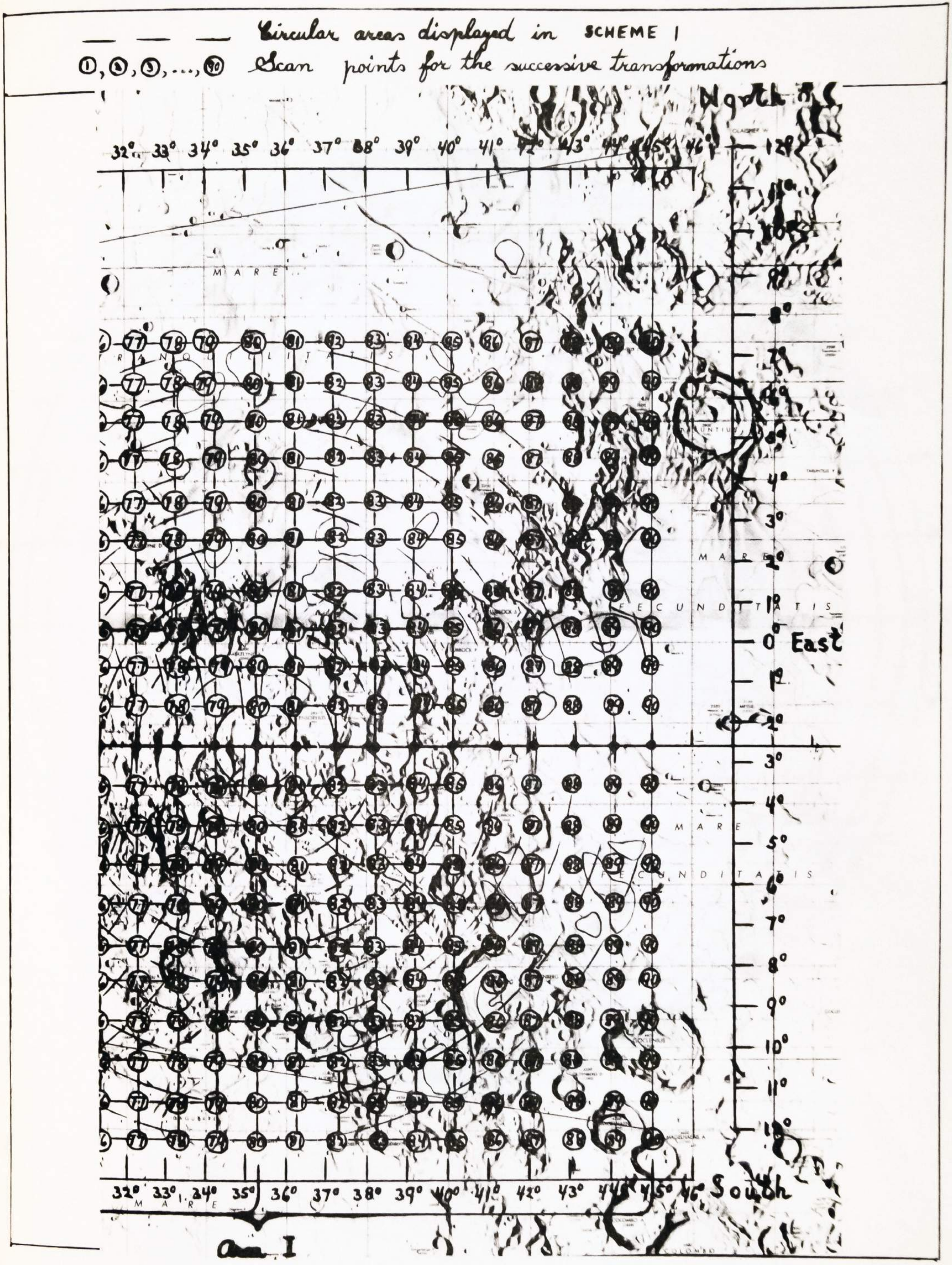

Map of the Moon Containing the Points To Be Observed, Whose Data Will Be Reduced by the Successive Transformation Method - Part V

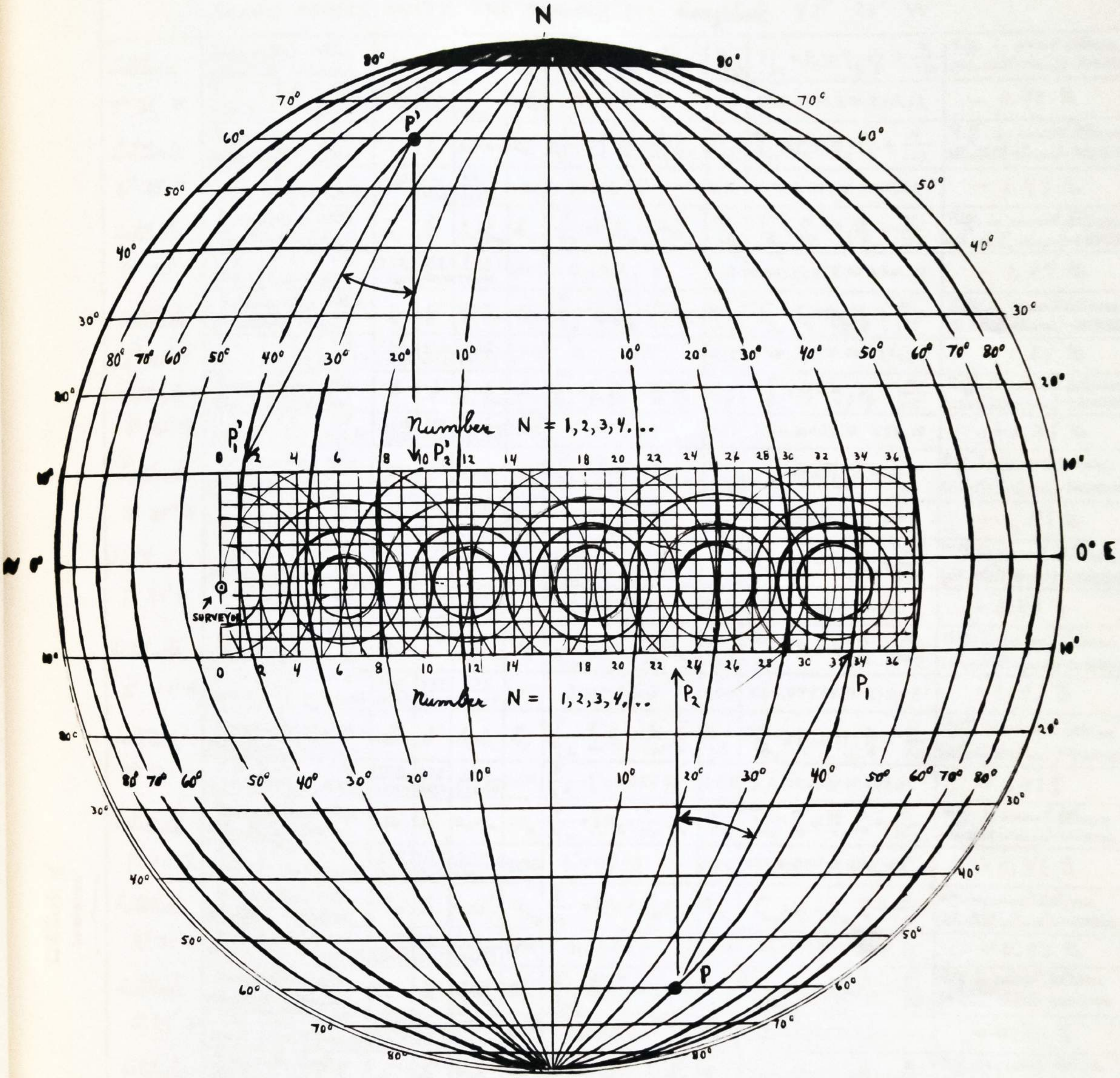

Scheme 5 - Correlation of the Number N of Successive Transformations Between the Mercator and Orthographic Projections

TABLE 2

Scans points of the overlapping concerning the areas A and B and their corresponding reduction

SCANS POINTS WITH THE NUMBER I : Longitude 42° 26' W

Latitude	Temperature after Shorthill-Saari			j	j'	$j_n = j^b$	j_x	$\frac{P}{\eta_j} = \sum j_x = \frac{14}{100} j_x$	η_j	$T_{j_x} = P_0 + \eta_j P_j + \frac{N}{100}$	Diff. in percent [redacted] (Shorthill-Saari)-[redacted]
7° 25' N	°K 386.4	°C 113.4	°F 236.12	$\frac{235}{236.12}$	$\frac{235}{214.5}$	$\frac{235}{236.12}$	0.916	0.12824	0.12	235.11992 ≈ 235.12	− 0.42 %
Latitude	Temperature after Shorthill-Saari			i	i'	$i_n = i$	i_x	$\frac{P}{\eta_i} = \sum i_x = \frac{13}{100} i_x$	η_i	$T_{i_x} = P_0 + \eta_i P_i + \frac{N}{100}$	Diff. in percent [redacted] (Shorthill-Saari)-[redacted]
6° 25' N	°K 387.7	°C 114.7	°F 238.46	$\frac{235}{238.46}$	$\frac{235}{202.[illegible]}$	$\frac{235}{238.46}$	0.847	0.11011	0.12	235,02321 ≈ 235.02	− 1.44 %
Latitude	Temperature after Shorthill-Saari			h	h'	$h_n = h_m$	h_x	$\frac{P}{\eta_h} = \sum h_x = \frac{12}{100} h_x$	η_h	$T_{h_x} = P_0 + \eta_h P_h + \frac{N}{100}$	Diff. in percent [redacted] (Shorthill-Saari)-[redacted]
5° 25' N	°K 388.3	°C 115.3	°F 239.54	$\frac{235}{239.54}$	$\frac{235}{245.12}$	$\frac{235}{232.95}$	1.024	0.12288	0.11	235.12264 ≈ 235.12	− 1.84 %
Latitude	Temperature after Shorthill-Saari			g	g'	$g_n = g_m$	g_x	$\frac{P}{\eta_g} = \sum g_x = \frac{11}{100} g_x$	η_g	$T_{g_x} = P_0 + \eta_g P_g + \frac{N}{100}$	Diff. in percent [redacted] (Shorthill-Saari)-[redacted]
4° 25' N	°K 388.3	°C 115.3	°F 239.54	$\frac{235}{239.54}$	$\frac{235}{245.12}$	$\frac{235}{232.95}$	1.024	0.11264	0.10	235.1124 ≈ 235.11	− 1.84 %
Latitude	Temperature after Shorthill-Saari			f	f'	$f_n = f_m$	f_x	$\frac{P}{\eta_f} = \sum f_x = \frac{10}{100} f_x$	η_f	$T_{f_x} = P_0 + \eta_f P_f + \frac{N}{100}$	Diff. in percent [redacted] (Shorthill-Saari)-[redacted]
3° 25' N	°K 387.7	°C 114.7	°F 238.46	$\frac{235}{238.46}$	$\frac{235}{244.04}$	$\frac{235}{232.95}$	1.024	0.10240	0.09	235.10216 ≈ 235.10	− 1.41 %
Latitude	Temperature after Shorthill-Saari			l	l'	$l_n = l_m$	l_x	$\frac{P}{\eta_l} = \sum l_x = \frac{9}{100} l_x$	η_l	$T_{l_x} = P_0 + \eta_l P_l + \frac{N}{100}$	Diff. in percent [redacted] (Shorthill-Saari)-[redacted]
2° 25' N	°K 387.7	°C 114.7	°F 238.46	$\frac{235}{234.95}$	$\frac{235}{242.96}$	$\frac{235}{232.95}$	1,034	0,09306	0,08	235,08272 ≈ 235,08	− 1.41 %
Latitude	Temperature after Shorthill-Saari			d	d'	$d_n = d_m$	d_x	$\frac{P}{\eta_d} = \sum d_x = \frac{8}{100} d_x$	η_x	$T_{d_x} = P_0 + \eta_d P_d + \frac{N}{100}$	Diff. in percent [redacted] (Shorthill-Saari)-[redacted]
1° 25' N	°K 387.7	°C 114.7	°F 238.46	$\frac{235}{238.46}$	$\frac{235}{240.62}$	$\frac{235}{232.95}$	1,009	0.08072	0,07	235,07063 ≈ 235,07	− 1.41 %
Latitude	Temperature after Shorthill-Saari			c	c'	$c_n = c_m$	c_x	$\frac{P}{\eta_c} = \sum c_x = \frac{7}{100} c_x$	η_c	$T_{c_x} = P_0 + \eta_c P_c + \frac{N}{100}$	Diff. in percent [redacted] (Shorthill-Saari)-[redacted]
0° 25' N	°K 387.7	°C 114.7	°F 238.46	$\frac{235}{238.46}$	$\frac{235}{240.62}$	$\frac{235}{232.95}$	1,009	0,07063	0,06	235,07054 ≈ 235,07	−1.41 %
Latitude	Temperature after Shorthill-Saari			b	b'	$b_n = b_m$	b_x	$\frac{P}{\eta_b} = \sum b_x = \frac{6}{100} b_x$	η_b	$T_{b_x} = P_0 + \eta_b P_b + \frac{N}{100}$	Diff. in percent [redacted] (Shorthill-Saari)-[redacted]
0° 25' S	°K 387.7	°C 114.7	°F 238.46	$\frac{235}{237.29}$	$\frac{235}{238.46}$	$\frac{235}{232.95}$	0,990	$\frac{P}{\eta_b} = \sum = 0,05940$	0.05	$T = 235,0595 \approx 235,06$	− 1.41 %
Latitude	Temperature after Shorthill-Saari			a	a'	$a_n = a_m$	a_x	$\frac{P}{\eta_a} = \sum a_x = \frac{5}{100} a_x$	η_a	$T_{a_x} = P_0 + \eta_a P_a + \frac{N}{100}$	Diff. in percent [redacted] (Shorthill-Saari)-[redacted]
1° 25' S	°K 386.4	°C 113.4	°F 236.12	$\frac{235}{237.29}$	$\frac{235}{236.12}$	$\frac{235}{232.95}$	0,996	0.04980	0.04	235,01984 ≈ 235.02	− 0.46 %
Latitude	Temperature after Shorthill-Saari			a_0	b_0	$a_0 = b_0$	a_{0_s}	$\frac{P}{a_0} = \sum a_0 = \frac{4}{100} a_0$	η_{a_0}	$T_{a_0} = P_0 + \eta_{a_0} P_{a_0} + \frac{N}{100}$	Diff. in percent [redacted] (Shorthill-Saari)-[redacted]
2° 25' S	°K 386.4	°C 113.4	°F 236.12	$\frac{235}{232.95}$	$\frac{235}{232.95}$	$\frac{235}{232.95}$	1,000	0.04000	0.03	235,01263 ≈ 235.01	− 0.42 %
Latitude	Temperature after Shorthill-Saari			a''	a'	$a''_n = b''_x$	a''_x	$\frac{P}{\eta_{a''}} = \sum a''_x = \frac{5}{100} a''_x$	$\eta_{a''}$	$T_{a''_x} = P_0 + \eta_{a''} P_{a''} + \frac{N}{100}$	Diff. in percent [redacted] (Shorthill-Saari)-[redacted]
3° 25' S	°K 386.4	°C 113.4	°F 236.12	$\frac{235}{236.12}$	$\frac{235}{236.12}$	$\frac{235}{236.12}$	0.995	0.04975	0.04	235.03985 ≈ 235.04	− 0.45 %
Latitude	Temperature after Shorthill-Saari			b''	b'	$b''_n = b''_s$	b''_x	$\frac{P}{\eta_{b''}} = \sum b''_x = \frac{6}{100} b''_x$	$\eta_{b''}$	$T_{b''_x} = P_0 + \eta_{b''} P_{b''} + \frac{N}{100}$	Diff. in percent [redacted] (Shorthill-Saari)-[redacted]
4° 25' S	°K 386.4	°C 113.4	°F 236.12	$\frac{235}{236.12}$	$\frac{236}{238.46}$	$\frac{235}{236.12}$	0,995	0.05970	0,05	235.05975 ≈ 235.06	− 0.44 %
Latitude	Temperature after Shorthill-Saari			c''	c'	$c''_n = c''_s$	c''_x	$\frac{P}{\eta_{c''}} = \sum c''_x = \frac{7}{100} c''_x$	$\eta_{c''}$	$T_{c''_x} = P_0 + \eta_{c''} P_{c''} + \frac{N}{100}$	Diff. in percent [redacted] (Shorthill-Saari)-[redacted]
5° 25' S	°K 386.4	°C 113.4	°F 236.12	$\frac{235}{238.46}$	$\frac{235}{240.62}$	$\frac{235}{236.12}$	1,065	0.07455	0.06	235.07390 ≈ 235.07	− 0.44 %
Latitude	Temperature after Shorthill-Saari			d''	d'	$d''_n = d''_s$	d''_x	$\frac{P}{\eta_{d''}} = \sum d''_x = \frac{8}{100} d''_x$	$\eta_{d''}$	$T_{d''_x} = P_0 + \eta_{d''} P_{d''} + \frac{N}{100}$	Diff. in percent [redacted] (Shorthill-Saari)-[redacted]
6° 25' S	°K 387.7	°C 114.7	°F 238.46	$\frac{235}{236.12}$	$\frac{235}{240.62}$	$\frac{235}{236.12}$	1.075	0.08600	0.07	235,08525 ≈ 235.08	−1.41 %

Latitude of SURVEYOR

TABLE 2 (continued)

Latitude	Temperature after Shorthill - Saari			ℓ''	ℓ'	$\ell''_n=\ell''_\sigma$	ℓ''_x	$\frac{P}{\eta_{\ell''}}=\sum \ell''_x=\frac{9}{100}\ell''_x$	$\eta_{\ell''}$	$T_{\ell''_x}=P_0+\eta_{\ell''}P_{\ell''}+\frac{N}{100}$	Diff. in percent b[redacted] (Shorthill-Saari)-S[redacted]
7° 25' S	°K 385.7	°C 112.7	°F 234.86	$\frac{235}{234.86}$	$\frac{235}{242.86}$	$\frac{235}{236.12}$	0.997	0.08973	0,08	235,08976 ≈ 235.09	+ 0.05 %
Latitude	Temperature after Shorthill - Saari			f''	f'	$f''_n=f''_\sigma$	f''_x	$\frac{P}{\eta_{f''}}=\sum f''_x=\frac{10}{100}f''$	$\eta_{f''}$	$T_{f''_x}=P_0+\eta_{f''}P_{f''}+\frac{N}{100}$	Diff. in percent b[redacted] (Shorthill-Saari)-S[redacted]
8° 25' S	°K 386.4	°C 113.4	°F 236.12	$\frac{235}{234.86}$	$\frac{235}{244.04}$	$\frac{235}{236.12}$	1.002	0, 10020	0.09	235.10018 ≈ 235.10	− 0.43 %
Latitude	Temperatung after Shorthill - Saari			g''	g'	$g''_n=g''_\sigma$	g''_x	$\frac{P}{\eta_{g''}}=\sum g''_x=\frac{11}{100}g''$	$\eta_{g''}$	$T_{g''_x}=P_0+\eta_{g''}P_{g''}+\frac{N}{100}$	Diff. in percent b[redacted] (Shorthill-Saari)-[redacted]
9° 25' S	°K 386.4	°C 113.4	°F 236,12	$\frac{235}{233.78}$	$\frac{235}{245.12}$	$\frac{235}{236.12}$	1.095	0.11506	0.10	235.11460 ≈ 235.11	− 0.42 %
Latitude	Temperature after Shorthill - Saari			h''	h'	$h''_n=h''_\sigma$	h''_x	$\frac{P}{\eta_{h''}}=\sum h''_x=\frac{12}{100}h''$	$\eta_{h''}$	$T_{h''_x}=P_0+\eta_{h''}P_{h''}+\frac{N}{100}$	Diff. in percent b[redacted] (Shorthill-Saari)-SU[redacted]
10° 25' S	°K 383.9	°C 110.9	°F 231.62	$\frac{235}{233.78}$	$\frac{235}{245.12}$	$\frac{235}{231.62}$	1.059	$\frac{P}{\eta_{h''}}=0.12708$	0.11	235,12649 ≈ 235.12	+ 1.02 %
Latitude	Temperature after Shorthill - Saari			i''	i'	$i''_n=i''_\sigma$	i''_x	$\frac{P}{\eta_{i''}}=\sum i''_x=\frac{13}{100}i''$	$\eta_{i''}$	$T_{i''_x}=P_0+\eta_{i''}P_{i''}+\frac{N}{100}$	Diff. in percent b[redacted] (Shorthill-Saari)-[redacted]
11° 25' S	°K 384.5	°C 111.5	°F 232.70	$\frac{235}{231.62}$	$\frac{235}{202.04}$	$\frac{235}{232.70}$	~~1.010~~ 0.898	0.11674	$\eta=0,12$	235,11776 ≈ 235.12	+ 1.03 %
Latitude	Temperature after Shorthill - Saari			j''	j'	$j''_n=j''_\sigma$	j''_x	$\frac{P}{\eta_{j''}}=\sum j''_x=\frac{14}{100}j''$	$\eta_{j''}$	$T_{j''_x}=P_0+\eta_{j''}P_{j''}+\frac{N}{100}$	Diff. in percent b[redacted] (Shorthill-Saari)[redacted]
12° 25' S	°K 386.4	°C 113.4	°F 236.12	$\frac{235}{232.7}$	$\frac{235}{214.5}$	$\frac{235}{236.12}$	1,000	0.13000	0.12	235.13000 = 235.13	− 0.42 %
	SCANS POINTS WITH THE NUMBER 2 : Longitude 41° 26' W										
Latitude	Temperature after Shorthill - Saari			j	j'	$j_n=j_m$	j_x	$\frac{P}{\eta_j}=\sum j_x=\frac{14}{100}j_x$	η_j	$T_{j_x}=P_0+\eta_j P_j+\frac{N}{100}$	Diff. in percent b[redacted] (Shorthill-Saari)-[redacted]
7° 25' N	°K 386.4	°C 113.4	°F 236.12	$\frac{235}{236.12}$	$\frac{235}{214.5}$	$\frac{235}{236.12}$	0.904	0.12656	0.12	235.12848 ≈ 235.13	− 0.42 %
Latitude	Temperature after Shorthill - Saari			i	i'	$i_n=i_m$	i_x	$\frac{P}{\eta_{i_x}}=\sum i_x=\frac{13}{100}i_x$	η_i	$T_{i_x}=P_0+\eta_i P_i+\frac{N}{100}$	Diff. in percent b[redacted] (Shorthill-Saari)-[redacted]
6° 25' N	°K 387.7	°C 114.7	°F 238.46	$\frac{235}{238.46}$	$\frac{235}{202.04}$	$\frac{235}{238.46}$	0.834	0.10842	0.11	235.11174 ≈ 235.11	− 1.40 %
Latitude	Temperature after Shorthill - Saari			h	h'	$h_n=h_m$	h_x	$\frac{P}{\eta_h}=\sum h_x=\frac{12}{100}h_x$	η_h	$T_{h_x}=P_0+\eta_h P_h+\frac{N}{100}$	Diff. in percent b[redacted] (Shorthill-Saari)-S[redacted]
5° 25' N	°K 388.9	°C 115.9	°F 240,62	$\frac{235}{239.54}$	$\frac{235}{245.12}$	$\frac{235}{240.62}$	1.000	0.12000	0.10	235.12000 = 235.12	− 2,28 %
Latitude	Temperature after Shorthill - Saari			g	g'	$g_n=g_m$	g_x	$\frac{P}{\eta_g}=\sum g_x=\frac{11}{100}g_x$	η_g	$T_{g_x}=P_0+\eta_g P_g+\frac{N}{100}$	Diff. in percent b[redacted] (Shorthill-Saari)-[redacted]
4° 25' N	°K 387.7	°C 114.7	°F 238.46	$\frac{235}{239.54}$	$\frac{235}{245.12}$	$\frac{235}{238.46}$	1,008	0.11088	0.09	235.09072 ≈ 235.09	− 1.41 %
Latitude	Temperature after Shorthill - Saari			f	f'	$f_n=f_m$	f_x	$\frac{P}{\eta_f}=\sum f_x=\frac{10}{100}f_x$	η_x	$T_{f_x}=P_0+\eta_f P_f+\frac{N}{100}$	Diff. in percent b[redacted] (Shorthill-Saari)-[redacted]
3° 25' N	°K 387.7	°C 114.7	°F 238.46	$\frac{235}{238.46}$	$\frac{235}{244.04}$	$\frac{235}{238.46}$	1,010	0.10101	0,08	235,10080 ≈ 235.10	− 1.41 %
Latitude	Temperature after Shorthill - Saari			ℓ	ℓ'	$\ell_n=\ell_m$	ℓ_x	$\frac{P}{\eta_\ell}=\sum \ell_x=\frac{9}{100}\ell_x$	η_ℓ	$T_{\ell_x}=P_0+\eta_\ell P_\ell+\frac{N}{100}$	Diff. in percent b[redacted] (Shorthill-Saari)-[redacted]
2° 25' N	°K 387.7	°C 114.7	°F 238.46	$\frac{235}{234.95}$	$\frac{235}{242.96}$	$\frac{235}{238.46}$	1,018	0.09162	0,07	235,11126 ≈ 235.11	− 1.44 %
Latitude	Temperature after Shorthill - Saari			d	d'	$d_n=d_m$	d_x	$\frac{P}{\eta_d}=\sum d_x=\frac{8}{100}d_x$	η_d	$T_{d_x}=P_0+\eta_d P_d+\frac{N}{100}$	Diff. in percent b[redacted] (Shorthill-Saari)-[redacted]
1° 25' N	°K 388.9	°C 115.9	°F 240,62	$\frac{235}{238.46}$	$\frac{235}{240.62}$	$\frac{235}{240.62}$	0.985	0.07880	0.06	235.07910 ≈ 235.08	− 2.30 %
Latitude	Temperature after Shorthill - Saari			c	c'	$c_n=c_m$	c_x	$\frac{P}{\eta_c}=\sum c_x=\frac{7}{100}c_x$	η_c	$T_{c_x}=P_0+\eta_c P_c+\frac{N}{100}$	Diff. in percent b[redacted] (Shorthill-Saari)[redacted]
0° 25' N	°K 388.9	°C 115.9	°F 240.62	$\frac{235}{238.56}$	$\frac{235}{240.62}$	$\frac{235}{240.62}$	0.985	0.06895	0.05	235.06925 ≈ 235.07	− 2.36

TABLE 2 (continued)

Latitude of SURVEYOR

Latitude	Temperature after Shorthill - Saari			b	b'	$b_n=b_m$	b_x	$\frac{P}{\eta_b}=\sum b_x=\frac{6}{100}b_x$	η_b	$T_{b_x}=P_0+\eta_b P_b+\frac{N}{100}$	Diff. in percent between (Shorthill-Saari)-SURVEYOR
0° 25' S	°K 388.9	°C 115.9	°F 240.62	$\frac{235}{237.29}$	$\frac{235}{238.40}$	$\frac{235}{240.62}$	0.981	0.05886	0.04	$^{235+}0.05924\approx 235.06$	− 2.31 %
Latitude	Temperature after Shorthill - Saari			a	a'	$a_n=a_m$	a_x	$\frac{P}{\eta_a}=\sum a_x=\frac{5}{100}a_x$	η_a	$T_{a_x}=P_0+\eta_a P_a+\frac{N}{100}$	Diff. in percent between (Shorthill-Saari)-SURVEYOR
1° 25' S	°K 388.9	°C 115.9	°F 240.62	$\frac{235}{237.29}$	$\frac{235}{236.12}$	$\frac{235}{240.62}$	0.971	0.04855	0.03	$235.04913\approx 235.05$	− 2.31 %
Latitude	Temperature after Shorthill - Saari			a_0	b_0	$a_0=b_0$	a_{0_S}	$\frac{P}{a_0}=\sum a_0=\frac{4}{100}a_0$	η_{a_0}	$T_{a_0}=P_0+\eta_{a_0}P_{a_0}+\frac{N}{100}$	Diff. in percent between (Shorthill-Saari)-SURVEYOR
2° 25' S	°K 388.3	°C 115.3	°F 239.54	$\frac{235}{232.95}$	$\frac{235}{232.95}$	$\frac{235}{239.54}$	1.008	0.04032	0.02	$235.06016\approx 235.06$	−1.87 %
Latitude	Temperature after Shorthill - Saari			a''	a'	$a''_n=a''_m$	a''_x	$\frac{P}{\eta_{a''}}=\sum a''_x=\frac{5}{100}a''_x$	$\eta_{a''}$	$T_{a''_x}=P_0+\eta_{a''}P_{a''}+\frac{N}{100}$	Diff. in percent between (Shorthill-Saari)-SURVEYOR
3° 25' S	°K 388.3	°C 115.3	°F 239.54	$\frac{235}{236.12}$	$\frac{235}{236.12}$	$\frac{235}{239.54}$	0.981	0.04905	0.03	$^{235+}0.04943\approx 235.05$	−1.87 %
Latitude	Temperature after Shorthill - Saari			b''	b'	$b''_n=b''_m$	b''_x	$\frac{P}{\eta_{b''}}=\sum b''_x=\frac{6}{100}b''_x$	$\eta_{b''}$	$T_{b''_x}=P_0+\eta_{b''}P_{b''}+\frac{N}{100}$	Diff. in percent between (Shorthill-Saari)-SURVEYOR
4° 25' S	°K 387.7	°C 114.7	°F 238.46	$\frac{235}{236.12}$	$\frac{235}{238.46}$	$\frac{235}{238.46}$	0.995	0.05970	0.04	$235.03980\approx 235.04$	− 1.43 %
Latitude	Temperature after Shorthill-Saari			c''	c'	$c''_n=c''_m$	c''_x	$\frac{P}{\eta_{c''}}=\sum c''_x=\frac{7}{100}c''_x$	$\eta_{c''}$	$T_{c''_x}=P_0+\eta_{c''}P_{c''}+\frac{N}{100}$	Diff. in percent between (Shorthill-Saari)-SURVEYOR
5° 25' S	°K 388.3	°C 115.3	°F 239.54	$\frac{235}{238.46}$	$\frac{235}{240.62}$	$\frac{235}{239.54}$	0.989	0.04945	0.05	$235.06945\approx 235.07$	− 1.81 %
Latitude	Temperature after Shorthill - Saari			d''	d'	$d''_n=d''_m$	d''_x	$\frac{P}{\eta_{d''}}=\sum d''_x=\frac{8}{100}d''_x$	$\eta_{d''}$	$T_{d''_x}=P_0+\eta_{d''}P_{d''}+\frac{N}{100}$	Diff. in percent between (Shorthill-Saari)-SURVEYOR
6° 25' S	°K 388.9	°C 115.9	°F 240.62	$\frac{235}{236.12}$	$\frac{235}{240.62}$	$\frac{235}{240.62}$	0.995	0.07960	0.06	$^{235+}0.07970\approx 235.08$	− 2.30 %
Latitude	Temperature after Shorthill - Saari			e''	e'	$e''_n=e''_m$	e''_x	$\frac{P}{\eta_{e''}}=\sum e''_x=\frac{9}{100}e''_x$	$\eta_{e''}$	$T_{e''_x}=P_0+\eta_{e''}P_{e''}+\frac{N}{100}$	Diff. in percent between (Shorthill-Saari)-SURVEYOR
7° 25' S	°K 388.3	°C 115.3	°F 239.54	$\frac{235}{234.86}$	$\frac{235}{242.86}$	$\frac{235}{239.54}$	1.014	0.09126	0.07	$235.09098\approx 235.09$	−1.85 %
Latitude	Temperature after Shorthill-Saari			f''	f'	$f''_n=f''_m$	f''_x	$\frac{P}{\eta_{f''}}=\sum f''_x=\frac{10}{100}f''_x$	$\eta_{f''}$	$T_{f''_x}=P_0+\eta_{f''}P_{f''}+\frac{N}{100}$	Diff. in percent between (Shorthill-Saari)-SURVEYOR
8° 25' S	°K 387.05	°C 114.05	°F 237.29	$\frac{235}{234.86}$	$\frac{235}{244.04}$	$\frac{235}{237.29}$	1.031	0.10310	0.08	$235.10248\approx 235.10$	− 0.92 %
Latitude	Temperature after Shorthill-Saari			g''	g'	$g''_n=g''_m$	g''_x	$\frac{P}{\eta_{g''}}=\sum g''_x=\frac{11}{100}g''_x$	$\eta_{g''}$	$T_{g''_x}=P_0+\eta_{g''}P_{g''}+\frac{N}{100}$	Diff. in percent between (Shorthill-Saari)-SURVEYOR
9° 25' S	°K 385.75	°C 112.7	°F 234.86	$\frac{235}{233.78}$	$\frac{235}{245.12}$	$\frac{235}{234.86}$	1.049	0.11539	0.09	$235.11441\approx 235.11$	+ 0.05 %
Latitude	Temperature after Shorthill-Saari			h''	h'	$h''_n=h''_m$	h''_x	$\frac{P}{\eta_{h''}}=\sum h''_x=\frac{12}{100}h''_x$	$\eta_{h''}$	$T_{h''_x}=P_0+\eta_{h''}P_{h''}+\frac{N}{100}$	Diff. in percent between (Shorthill-Saari)-SURVEYOR
10° 25' S	°K 383.9	°C 110.9	°F 231.62	$\frac{235}{233.78}$	$\frac{235}{245.12}$	$\frac{235}{231.62}$	1.014	0.12168	0.10	$^{235+}0.12014\approx 235.12$	+ 1.02 %
Latitude	Temperature after Shorthill-Saari			i''	i'	$i''_n=i''_m$	i''_x	$\frac{P}{\eta_{i''}}=\sum i''_x=\frac{13}{100}i''_x$	$\eta_{i''}$	$T_{i''_x}=P_0+\eta_{i''}P_{i''}+\frac{N}{100}$	Diff. in percent between (Shorthill-Saari)-SURVEYOR
11° 25' S	°K 384.5	°C 111.5	°F 232.70	$\frac{235}{234.62}$	$\frac{235}{202.04}$	$\frac{235}{232.70}$	0.868	0.11284	0.11	$235.11548\approx 235.11$	+ 1.01 %
Latitude	Temperature after Shorthill - Saari			j''	j'	$j''_n=j''_m$	j''_x	$\frac{P}{\eta_{j''}}=\sum j''_x=\frac{14}{100}j''_x$	$\eta_{j''}$	$T_{j''_x}=P_0+\eta_{j''}P_{j''}+\frac{N}{100}$	Diff. in percent between (Shorthill-Saari)-SURVEYOR
12° 25' S	°K 383.9	°C 110.9	°F 231.62	$\frac{235}{232.7}$	$\frac{235}{214.5}$	$\frac{235}{231.62}$	0.922	0.12908	0.12	$235.13064\approx 235.13$	+ 1.51 %

SCANS POINTS WITH THE NUMBER 3 ; Longitude 40° 26' W

Latitudes	Temperatures after Shorthill-Saari			$\bar{''}$	$'$	$\overset{''}{'}_n \; \overset{m}{\emptyset}$	x	$\frac{P}{\eta_x}=\sum x=\frac{x}{100}X$	η_x	$T_x=P_0+\eta_x P_x+\frac{N}{100}$	Differences (Shorthill-Saari)-SURVEYOR
7° 25' N	387.05	114.05	237.29	0.995	1.095	0.990	0.899	0.12586	0.11	$T_x=235.12889\approx 235.13$	− 0.91 %
6° 25' N	387.7	114.7	238.46	0.985	1.163	0.842	0.985	0.10946	0.10	$235.11420\approx 235.11$	− 1.40 %
5° 25' N	387.7	114.7	238.46	0.981	0.958	0.985	1.008	0.12096	0.09	$235.12072\approx 235.12$	− 1.40 %
4° 25' N	387.7	114.7	238.56	0.981	0.958	0.985	1.008	0.11088	0.08	$235.11064\approx 235.11$	− 1.40 %

TABLE 2 (continued)

3° 25' N	°K 388.9	°C 115.9	°F 240.62	0.985	0.960	0.971	0.995	0.09950	0.07	235.09965≈235.10	-2.34 %
2° 25' N	°K 388.9	°C 115.9	°F 240.62	1.000	0.967	0.971	1.004	0.09036	0.06	235.06024≈235.06	-2.31 %
1° 25' N	°K 388.9	°C 115.9	°F 240.62	0.985	0.976	0.971	0.980	0.07840	0.05	235.07900≈235.08	-2.30 %
0° 25' N	°K 388.9	°C 115.9	°F 240.62	0.985	0.976	0.971	0.980	0.06860	0.04	235.06920≈235.07	-2.30 %
0° 25' S	°K 389.5	°C 116.5	°F 241.7	0.990	0.985	0.972	0.978	0.05868	0.03	235.05934≈235.06	-2.74 %
1° 25' S	°K 388.3	°C 115.3	°F 239.54	0.990	0.995	0.981	0.985	0.04925	0.02	235.04970≈235.05	-1.87 %
Latitude of SURVEYOR→ 2° 25' S	°K 388.9	°C 115.9	°F 240.62	1.008	1.008	0.971	0.971	0.03884	0.01	235.00971≈235.01	-2.33 %
3° 25' S	°K 387.7	°C 114.7	°F 238.46	0.995	0.995	0.985	0.985	0.04925	0.02	235.04970≈235.05	-1.42 %
4° 25' S	°K 388.9	°C 115.9	°F 240.62	0.995	0.985	0.971	0.981	0.05886	0.03	235.05943≈235.06	-2.31 %
5° 25' S	°K 388.9	°C 115.9	°F 240.62	0.985	0.976	0.971	0.980	0.06860	0.04	235.06920≈235.07	-2.31 %
6° 25' S	°K 388.9	°C 115.9	°F 240.62	0.995	0.976	0.971	0.989	0.07912	0.05	235.07945≈235.08	-2.30 %
7° 25' S	°K 388.3	°C 115.3	°F 239.54	1.000	0.967	0.981	1.014	0.09126	0.06	235.06084≈235.06	-1.87 %
8° 25' S	°K 388.3	°C 115.3	°F 239.54	1.000	0.967	0.981	1.014	0.10140	0.07	235.07098≈235.07	-1.86 %
9° 25' S	°K 387.7	°C 114.7	°F 238.46	1.005	0.958	0.985	1.028	0.11308	0.08	235.11224≈235.11	-1.40 %
10° 25' S	°K 385.1	°C 112.1	°F 233.78	1.005	0.958	1.005	1.043	0.12516	0.09	235.12045≈235.12	+0.57 %
11° 25' S	387.05	114.05	237.29	1.010 ~~0.990~~	1.163	0.990	0.951 ~~1.163~~	0.11063	0.10	235.11510≈235.11	-0.96 %
12° 25' S	°K 387.7	°C 114.7	°F 238.46	1.009	1.095	0.985	0.994	0.13916	0.11	235.13934≈235.14	-1.41 %
		SCANS POINTS WITH THE NUMBER								4 : Longitude	39° 26' W
Latitudes	Temperatures after Shorthill-Saari			¯ "	,	" m , n σ	X	$\frac{P}{\eta_x} = \sum x = \frac{x}{100} X$	η_x	$T_x = P_0 + \eta_x P_x + \frac{N}{100}$	Differences (Shorthill-Saari) - SURVEYOR
7° 25' N	°K 387.7	°C 114.7	°F 238.46	0.995	1.095	0.985	0.980	0.13720	0.10	235 0.03800≈235.14	-1.39 %
6° 25' N	°K 388.9	°C 115.9	°F 240.62	0.985	1.163	0.976	0.826	0.10738	0.09	235.11434≈235.11	-2.33 %
5° 25' N	°K 388.9	°C 115.9	°F 240.62	0.981	0.958	0.976	1.000	0.11484	0.08	235.12000≈235.12	-2.33 %
4° 25' N	°K 387.65	°C 114.65	°F 238.39	0.981	0.958	0.985	1.008	0.11088	0.07	235.11056≈235.11	-1.46 %
3° 25' N	388.3	115.3	239.54	0.985	0.960	0.981	1.006	0.09054	0.06	235.10036≈235.10	-1.84 %
2° 25' N	388.9	115.9	240.62	1.000	0.967	0.976	1.009	0.09081	0.05	235.09045≈235.09	-2.29 %
1° 25' N	389.55	116.55	241.75	0.985	0.976	0.972	0.957	0.07656	0.04	235.07656≈235.08	-2.76 %
0° 25' N	388.3	115.3	239.54	0.985	0.976	0.981	0.966	0.06762	0.03	235.06898≈235.07	-1.86 %
0° 25' S	389.55	116.55	241.75	0.990	0.985	0.972	0.995	0.05970	0.02	235.05990≈235.06	-2.77 %
1° 25' S	389.55	116.55	241.75	0.990	0.995	0.972	0.976	0.04880	0.01	235.04976≈235.05	-2.77 %
Latitude of SURVEYOR→ 2° 25' S	389.55	116.55	241.75	1.008	1.008	0.972	0.972	0.03888	0.01	235.04972≈235.05	-2.77 %
3° 25' S	389.55	116.55	241.75	0.995	0.995	0.972	0.972	0.04880	0.01	235.04976≈235.05	-2.77 %
4° 25' S	[illegible]	[illegible]	[illegible]	[illegible]	[illegible]	0.972	0.982	0.05892	0.02	[illegible]≈235.06	-2.77 %

TABLE 2 ([illegible])

5° 25' S	°K 389,55	°C 116,55	°F 241,75	0,985	0.976	0.972	0,981	0.06867	0.03	235.06943≈235.07	– 2.76 %
7° 25' S	°K 389,55	°C 116,55	°F 241,75	0,995	0,976	0.980	0,980	0.06860	0.04	235.07920≈235.08	– 2.76 %
8° 25' S	°K 389,55	°C 116.55	°F 241,75	1,000	0.967	0.972	1.005	0.10050	0.05	235.09025≈235.09	– 2.75 %
9° 25' S	°K 388.3	°C 115.3	°F 239.54	1,000	0.960	0.981	1,022	0.11242	0,06	235.10132≈235.10	– 1.84 %
10° 25' S	°K 388.3	°C 115,3	°F 239.54	1,005	0,958	0,981	1,029	0.12348	0,07	235.11213≈235.11	–1.84 %
11° 25' S	°K 388.3	°C 115.3	°F 239.54	1,005	0,958	0.981	1.029	0.13377	0.08	235.11848≈235.12	–1.84 %
12° 25' S	°K 388.3	°C 115,3	°F 239.54	1,009	1,095	0.981	0,905	0.12670	0,09	235.15383≈235.15	–1.83 %
6° 25' S	°K 388.3	°C 116.3	°F 239.54	1,000	0.960	0.981	1,022	0.08176	0.04	235.08088≈235.08	–1.86 %

SCANS POINTS WITH THE NUMBER 5 : *Longitude* 38° 26' W

Latitudes	*Temperatures after Shorthill-Saari*			— ”	›	” m , n σ	x	$\frac{P}{\eta_x}=\sum x=\frac{x}{100}X$	η_x	$T_x=P_0+\eta_x P_x+\frac{N}{100}$	*Differences*
7° 25' N	°K 387.7	°C 114.7	°F 238.46	0.995	1.095	0,985	0,980	0.16660	0.12	235.16760≈235.17	–1, 38 %
6° 25' N	°K 387.7	°C 114.7	°F 238.46	0.985	1,163	0,985	0.842	0.13472	0.11	235.14262≈235.14	–1, 39 %
5° 25' N	°K 387.7	°C 114.7	°F 238.46	0.981	0.958	0,985	1.008	0.15120	0.10	235.15080≈235.15	–1, 39 %
4° 25' N	°K 387.7	°C 114.7	°F 238.46	0,981	0.958	0.985	1.008	0.14112	0.09	235.14072≈235.14	–1. 39 %
3° 25' N	°K 387.7	°C 114.7	°F 238.46	0.985	0.960	0.985	1.010	0.12805	0,08	235.13080≈235.13	–1, 39 %
2° 25' N	°K 390,2	°C 117.2	°F 242.96	1.000	0.967	0,967	1.000	0.12000	0.07	235.12000=235.12	– 3, 22 %
1° 25' N	°K 390,2	°C 117.2	°F 242.96	0.985	0.976	0.967	0.975	0.10725	0.06	235.10850≈235.11	–3, 22 %
0° 25' N	°K 391.4	°C 118.4	°F 245.12	0.985	0.976	0.904	0.912	0.09120	0.05	235.09560≈235.10	– 4.09 %
0° 25' S	°K 390.2	°C 117.2	°F 242.96	0,990	0.985	0.967	0.971	0.08739	0.04	235.08884≈235.09	– 3,24 %
1° 25' S	°K 390.2	°C 117.2	°F 242.96	0.990	0.995	0.967	0,971	0.07768	0.03	235,07913≈235,08	– 3, 24 %
Latitude of SURVEYOR → 2° 25' S	°K 390,2	°C 117.2	°F 242.96	1.008	1.008	0.967	0.967	0.06769	0.02	235.06934≈235.07	– 3.24 %
3° 25' S	°K 388,9	°C 115.9	°F 240.62	0.995	0.995	0.971	0.971	0.07768	0.03	235.07913≈235.08	– 2.30 %
4° 25' S	°K 388.9	°C 115.9	°F 240.62	0.995	0.985	0,971	0.981	0.08829	0.04	235.08924≈235.09	– 2.30 %
5° 25' S	°K 390.2	°C 117.2	°F 242.96	0.985	0.976	0.967	0.976	0.09760	0.05	235,09880≈235,10	– 3, 23 %
6° 25' S	°K 390.2	°C 117.2	°F 242.96	0.995	0.976	0.967	0.985	0.10835	0.06	235.10910≈235.11	– 3, 23 %
7° 25' S	°K 388.9	°C 115.9	°F 240.62	1.000	0.967	0.971	1,004	0,12048	0.07	235.12028≈235,12	– 2, 28 %
8° 25' S	°K 388.9	°C 115.9	°F 240.62	1.000	0.960	0,971	1,012	0.13156	0.08	235.13096≈235,13	– 2, 28 %
9° 25' S	°K 388.9	°C 115.9	°F 240.62	1.005	0.958	0.971	1.017	0.14238	0.09	235.14153≈235.14	– 2. 28 %
10° 25' S	°K 389.55	°C 116,55	°F 241.75	1.005	0.958	0.972	1.017	0.15255	0.10	235.15170≈235.15	–2.73 %
11° 25' S	°K 389.55	°C 116,55	°F 241,75	1.010	1.163	0.972	0.842	0.13472	0.11	235.14262≈235.14	– 2.73 %
12° 25' S	°K [illegible]	°C [illegible]	°F [illegible]	1,009	1,095	0.972	0.895	0.16824	0.12	[illegible].16824≈[illegible]	–2.73 %

TABLE 2 (continued)

SCANS POINTS WITH THE NUMBER 6 : Longitude 37° 26' W

Latitudes	Temperatures after Shorthill-Saari			$\overline{,,}$	,	,, m , n σ	X	$\frac{P}{\eta_x}=\sum x=\frac{x}{100}X$	η_x	$T_x=P_0+\eta_x P_x+\frac{N}{100}$	Differences
7° 25' N	°K 386.4	°C 113.4	°F 236.12	0.995	1,095	0,985	0.916	0.15572	0.11	235.16076≈235.16	-0.40 %
6° 25' N	°K 386.4	°C 113.4	°F 236.12	0.985	1.163	0.985	0.834	0.13344	0.10	235.14340≈235.14	-0.41 %
5° 25' N	°K 387.7	°C 114.7	°F 238.46	0.981	0.958	0.985	1,008	0.15120	0,09	235.15072≈235,15	-0.40 %
4° 25' N	°K 388.9	°C 115.9	°F 240.62	0.981	0.958	0.971	0.993	0.13902	0.08	235.13944≈235,14	-2.27 %
3° 25' N	°K 390.2	°C 117.2	°F 242.96	0.985	0.960	0.967	0.981	0.10753	0.07	235.12867≈235.13	-3.22 %
2° 25' N	°K 390.2	°C 117.2	°F 242.96	1.000	0.967	0.967	1.000	0.12000	0.06	235.12000≈235.12	-3,22 %
1° 25' N	390.2	117.2	242.96	0.985	0.976	0.967	0.975	0.10725	0.05	235,10875≈235,11	-3.22 %
0° 25' N	°K 390.2	°C 117.2	°F 242.96	0.985	0.976	0.967	0,975	0,09750	0.04	235,09900≈235,10	-3.23 %
0° 25' S	°K 390.2	°C 117.2	°F 242.96	0.990	0.985	0.967	0.972	0,08748	0.03	235.08916≈235.09	-3.23 %
1° 25' S	°K 390.2	°C 117.2	°F 242.96	0.990	0.995	0.967	0.982	0.078856	0.02	235,07964≈235,08	-3.23 %
2° 25' S	°K 390.2	°C 117.2	°F 242.96	1.008	1.008	0.967	0.959	0.06713	0.01	235.06959≈235.07	-3.23 %
3° 25' S	°K 390.2	°C 117.2	°F 242.96	0.995	0.995	0.967	0.967	0.07736	0.02	235.07934≈235.08	-3.23 %
4° 25' S	°K 390.2	°C 117.2	°F 242.96	0.995	0.985	0.967	0.978	0.08784	0.03	235.08928≈235.09	-3.23 %
5° 25' S	°K 390.2	°C 117.2	°F 242.96	0.985	0.976	0.967	0.952	0.09520	0.04	235.09808≈235.10	-3,23 %
6° 25' S	°K 390.2	°C 117.2	°F 242.96	0.995	0.976	0.967	0.976	0.10736	0.05	235.10880≈235.11	-3,23 %
7° 25' S	°K 390.2	°C 117.2	°F 242.96	1.000	0.967	0.967	1.000	0.12736	0.06	235.12000≈235.12	-3.23 %
8° 25' S	°K 390.2	°C 117.2	°F 242.96	1.000	0.960	0.967	1.007	0.13091	0.07	235.13049≈235.13	-3,23 %
9° 25' S	°K 390.2	°C 117.2	°F 242.96	1.005	0.958	0.967	1,014	0.14196	0.08	235.14196≈235,14	-3, 23 %
10° 25' S	°K 390.2	°C 117.2	°F 242.96	1.005	0.958	0.967	1.014	0.15210	0.09	235.15126≈235,15	-3, 21 %
11° 25' S	°K 390.2	°C 117.2	°F 242.96	1.010	1.163	0.967	0.839	0.13424	0.10	235.14390≈235.14	-3, 21 %
12° 25' S	°K 390.2	°C 117.2	°F 242.96	1,009	1,095	0.967	0.890	0.15130	0.11	235.15790≈235.16	-3.21 %
	SCANS POINTS WITH THE NUMBER								7 :	Longitude 36°	26' W
7° 25' N	°K 387.7	°C 114.7	°F 238.46	0.995	1.095	0,985	0.980	0.16660	0.10	235.16800≈235.17	-1.37 %
6° 25' N	°K 390.2	°C 117.2	°F 242.96	0.985	1.163	0.967	0.818	0.13088	0.09	235.14362≈235,14	-3, 22 %
5° 25' N	°K 390.2	°C 117.2	°F 242.96	1.005	0.958	0.967	0.972	0.14362	0.08	235.14776≈235.15	-3, 22 %
4° 25' N	°K 390.2	°C 117.2	°F 242.96	0.981	0.958	0.967	0.989	0.13846	0.07	235.13923≈235.14	-3, 22 %
3° 25' N	°K 390.2	°C 117.2	°F 242.96	0.985	0.960	0.967	0.981	0.12753	0.06	235.12886≈235.13	-3.22 %
2° 25' N	°K 390.2	°C 117.2	°F 242.96	1.000	0.967	0.967	1.000	0.12753	0.05	235.12000≈235.12	-3. 22 %
1° 25' N	°K [illegible]	°C [illegible]	°F [illegible]	[illegible]	0.976	0.967	0.965	0.10615	0.04	235.10860≈235.11	-3, 22 %

Latitude of SURVEYOR →

TABLE 2 (continued)

0° 25' N	°K 390.2	°C 117.2	°F 242.96	0.985	0.976	0.967	0.965	0.09650	0.03	235.09895≈235.10	-3.22 %
0° 25' S	°K 390.8	°C 117.8	°F 244.04	0.990	0.985	0.963	0.967	0.08703	0.02	235.08934≈235.09	-3.66 %
1° 25' S	°K 390.8	°C 117.8	°F 244.04	0.990	0.995	0.963	0.958	0.07664	0.01	235.07958≈235.08	-3.66 %
Latitude of [illegible]→ 2° 25' S	°K 391.4	°C 118.4	°F 245.12	1.008	1.008	0.958	0.958	0.06706	0.01	235.07958≈235.08	-4.09 %
3° 25' S	°K 391.4	°C 118.4	°F 245.12	0.995	0.995	0.958	0.958	0.07664	0.01	235.07958≈235.08	-4.09 %
4° 25' S	°K 391.4	°C 118.4	°F 245.12	0.995	0.985	0.958	0.967	0.08703	0.02	235.08934≈235.09	-4.09 %
5° 25' S	°K 390.2	°C 117.2	°F 242.96	0.985	0.976	0.967	0.975	0.09750	0.03	235.09925≈235.10	-3.22 %
6° 25' S	°K 390.2	°C 117.2	°F 242.96	0.995	0.976	0.967	0.985	0.10835	0.04	235.10940≈235.11	-3.22 %
7° 25' S	°K 390.2	°C 117.2	°F 242.96	1.000	0.967	0.967	1.000	0.12000	0.05	235.12000≈235.12	-3.22 %
8° 25' S	°K 390.2	°C 117.2	°F 242.96	1.000	0.960	0.967	1.007	0.13091	0.06	235.13042≈235.13	-3.22 %
9° 25' S	°K 390.8	°C 117.8	°F 244.04	1.005	0.958	0.962	1.008	0.14112	0.07	235.14056≈235.14	-3.64 %
10° 25' S	°K 390.8	°C 117.8	°F 244.04	1.005	0.958	0.962	1.008	0.15120	0.08	235.15064≈235.15	-3.64 %
11° 25' S	°K 391.4	°C 118.4	°F 245.12	1.010	1.163	0.958	0.829	0.13264	0.09	235.14461≈235.14	-4.07 %
12° 25' S	°K 390.8	°C 117.8	°F 244.04	1.009	1.095	0.962	0.885	0.14945	0.10	235.15850≈235.16	-3.64 %

SCANS POINTS WITH THE NUMBER 8 : Longitude 35° 26' W

Latitudes	Temperatures after Shorthill–Saari			$\overline{''}$	'	n m n σ	x	$\frac{P}{\eta_x} = \sum x = \frac{x}{100} X$	η_x	$T_x = P_0 + \eta_x P_x + \frac{N}{100}$	Differences
7° 25' N	°K 390.2	°C 117.2	°F 242.96	0.995	1.009	0.967	0.952	0.19040	0.12	235.19424≈235.19	-3.19 %
6° 25' N	°K 390.2	°C 117.2	°F 242.96	0.985	1.103	0.967	0.818	0.15542	0.11	235.16998≈235.17	-3.20 %
5° 25' N	°K 390.2	°C 117.2	°F 242.96	0.981	0.958	0.967	0.987	0.17766	0.10	235.17870≈235.18	-3.20 %
4° 25' N	°K 388.9	°C 115.9	°F 240.62	0.981	0.958	0.971	0.993	0.16881	0.09	235.16937≈235.17	-2.26 %
3° 25' N	°K 390.2	°C 117.2	°F 242.96	0.985	0.960	0.967	0.992	0.15872	0.08	235.15936≈235.16	-3.21 %
2° 25' N	°K 390.2	°C 117.2	°F 242.96	1.000	0.967	0.967	1.000	0.15000	0.07	235.15000=235.15	-3.21 %
1° 25' N	°K 390.2	°C 117.2	°F 242.96	0.985	0.976	0.967	0.976	0.13650	0.06	235.13856≈235.13	-3.22 %
0° 25' N	°K 390.2	°C 117.2	°F 242.96	0.985	0.976	0.967	0.976	0.12688	0.05	235.12880≈235.13	-3.22 %
0° 25' S	°K 391.4	°C 118.4	°F 245.12	0.990	0.985	0.958	0.952	0.11424	0.04	235.11808≈235.12	-4.07 %
1° 25' S	390.2	117.2	242.96	0.990	0.995	0.967	0.965	0.10615	0.03	235.10895≈235.11	-3.23 %
Latitude of SURVEYOR→ 2° 25' S	390.2	117.2	242.96	1.008	1.008	0.967	0.967	0.09670	0.02	235.09934≈235.10	-3.2[illegible] %
3° 25' S	391.4	118.4	245.12	0.995	0.995	0.958	0.958	0.10538	0.03	235.10874≈235.11	-4.07 %
4° 25' S	391.4	118.4	245.12	0.995	0.985	0.958	0.968	0.11616	0.04	235.11872≈235.12	-4.0[illegible] %
5° 25' S	391.4	118.4	245.12	0.985	0.976	0.958	0.968	0.12571	0.05	235.12840≈235.13	-4.0[illegible] %
6° 25' S	391.4	118.4	245.12	0.995	0.976	0.958	0.976	0.13664	0.06	235.13856≈235.14	-4.0[illegible] %
7° 25' S	391.4	118.4	245.12	1.000	0.967	0.958	0.991	0.14865	0.07	235.14937≈235.15	-4.0[illegible] %
8° 25' S	391.4	118.4	245.12	1.000	0.960	0.958	0.998	0.15978	0.08	235.15984≈235.16	-4.06 %
9° 25' S	390.8	117.8	244.04	1.005	0.958	0.962	1.009	0.17153	0.09	235.17081≈235.17	-3.64 %
10° 25' S	390.8	117.8	244.04	1.005	0.958	0.962	1.009	0.18162	0.10	235.18090≈235.18	-3.64 %
11° 25' S	390.8	117.8	244.04	1.010	1.163	0.962	0.921	0.17499	0.11	235.18131≈235.18	-3.64 %
12° 25' S	390.8	117.8	244.04	1.009	[illegible]	0.962	0.978	0.19560	0.12	235.197[illegible]	-3.62 %

TABLE 2 (continued)

SCANS POINTS WITH THE NUMBER 9 : Longitude 34° 26' W

Latitudes	Temperatures after Shorthill - Saari			— »	›	» m n σ	x	$\frac{P}{\eta_x}=\sum x=\frac{x}{100}X$	η_x	$T_x=P_0+\eta_xP_x+\frac{N}{100}$	Differences
7° 25' N	°K 390.2	°C 117.2	°F 242.96	0.995	1.009	0.967	0.952	0.19040	0.11	235.19472≈235.19	-3.19
6° 25' N	°K 390.2	°C 117.2	°F 242.96	0.985	1.163	0.967	0.818	0.15542	0.10	235.17180≈235.17	-3.20
5° 25' N	°K 390.2	°C 117.2	°F 242.96	0.981	0.958	0.967	0.987	0.17766	0.09	235.17883≈235.18	-3.20
4° 25' N	°K 390.2	°C 117.2	°F 242.96	0.981	0.958	0.967	0.987	0.16779	0.08	235.16896≈235.17	-3.20
3° 25' N	°K 390.2	°C 117.2	°F 242.96	0.985	0.960	0.967	0.992	0.15872	0.07	235.15944≈235.16	-3.21
2° 25' N	°K 390.2	°C 117.2	°F 242.96	1.000	0.967	0.967	1.000	0.15000	0.06	235.15000≈235.15	-3.21
1° 25' N	°K 390.2	°C 117.2	°F 242.96	0.985	0.976	0.967	0.976	0.13650	0.05	235.13880≈235.14	-3.22
0° 25' N	°K 390.2	°C 117.2	°F 242.96	0.985	0.976	0.967	0.976	0.12688	0.04	235.12904≈235.13	-3.22
1° 25' S	391.4	118.4	245.12	0.990	0.995	0.958	0.952	0.10472	0.03	235.11856≈235.12	-4.07
Latitude of SURVEYOR→ 2° 25' S	391.4	118.4	245.12	1.008	1.008	0.958	0.958	0.09580	0.02	235.10916≈235.11	-4.07
3° 25' S	391.4	118.4	245.12	0.995	0.995	0.958	0.958	0.10538	0.03	235.11874≈235.12	-4.07
4° 25' S	390.8	117.8	244.04	0.995	0.985	0.962	0.974	0.11688	0.04	235.12896≈235.13	-3.65
5° 25' S	390.8	117.8	244.04	0.985	0.976	0.962	0.970	0.12610	0.05	235.13850≈235.14	-3.65
6° 25' S	391.4	118.4	245.12	0.995	0.976	0.958	0.976	0.13664	0.06	235.14856≈235.15	-4.07
7° 25' S	391.4	118.4	245.12	1.000	0.967	0.958	0.991	0.14865	0.07	235.15937≈235.16	-4.07
8° 25' S	391.4	118.4	245.12	1.000	0.960	0.958	0.998	0.15968	0.08	235.16984≈235.17	-4.07
9° 25' S	391.4	118.4	245.12	1.005	0.958	0.958	1.005	0.17085	0.09	235.18045≈235.18	-4.05
10° 25' S	391.4	118.4	245.12	1.005	0.958	0.958	1.005	0.18090	0.10	235.19050≈235.19	-4.0[illegible]
11° 25' S	391.4	118.4	245.12	1.010	1.163	0.958	0.831	0.15789	0.11	235.18141≈235.18	-4.0[illegible]
12° 25' S	391.4	118.4	245.12	1.009	1.095	0.958	0.882	0.17640	0.12	235.19584≈235.20	
SCANS POINTS WITH THE NUMBER 10 : Longitude 33° 26' W											
7° 25' N	390.2	117.2	242.96	0.995	1.009	0.967	0.952	0.19040	0.10	235.19520≈235.20	-3.19
6° 25' N	388.9	115.9	240.62	0.985	1.163	0.971	0.822	0.15618	0.09	235.17398≈235.17	-2.26
5° 25' N	391.4	118.4	245.12	0.981	0.958	0.958	0.980	0.17640	0.08	235.17840≈235.18	-2.26
4° 25' N	390.2	117.2	242.96	0.981	0.958	0.967	0.989	0.16813	0.07	235.16923≈235.17	-3.20
3° 25' N	390.2	117.2	242.96	0.985	0.960	0.967	0.992	0.15872	0.06	235.15952≈235.16	-3.21
2° 25' N	390.2	117.2	242.96	1.000	0.967	0.967	1.000	0.15000	0.05	235.15000≈235.15	-3.21
1° 25' N	390.2	117.2	242.96	0.985	0.976	0.967	0.976	0.13650	0.04	235.13904≈235.14	-3.21
0° 25' N	390.2	117.2	242.96	0.985	0.976	0.967	0.976	0.12688	0.03	235.12928≈235.13	-3.21
0° 25' S	391.4	118.4	245.12	0.990	0.985	0.958	0.952	0.11424	0.02	235.11904≈235.12	-4.07
1° 25' S	391.4	118.4	245.12	0.990	0.995	0.958	0.952	0.10472	0.01	235.10952≈235.11	-4.07
Latitude of SURVEYOR→ 2° 25' S	390.8	117.8	244.04	1.008	1.008	0.962	0.962	0.09620	0.01	235.10962≈235.11	-3.65
3° 25' S	391.4	118.4	245.12	0.995	0.995	0.958	0.958	0.10538	0.01	235.10958≈235.11	-4.07
4° 25' S	391.4	118.4	245.12	0.995	0.985	0.958	0.968	0.11616	0.02	235.11930≈235.12	-4.07
5° 25' S	390.2	117.2	242.96	0.985	0.976	0.967	0.976	0.09760	0.03	235.12928≈235.13	-3.2[illegible]
6° 25' S	390.2	117.2	242.96	0.995	0.976	0.967	0.985	0.10835	0.04	235.13940≈235.14	-3.2[illegible]
7° 25' S	391.4	118.4	245.12	1.000	0.967	0.958	0.991	0.14865	0.05	235.14955≈235.15	-4.06
8° 25' S	391.4	118.4	245.12	1.000	0.960	0.958	0.998	0.15978	0.06	235.15988≈235.16	-4.06
9° 25' S	391.4	118.4	245.12	1.005	0.958	0.958	1.005	0.17085	0.07	235.17035≈235.17	-4.06
10° 25' S	391.4	118.4	245.12	1.005	0.958	0.958	1.005	0.18090	0.08	235.18040≈235.18	-4.06
11° 25' S	391.4	118.4	245.12	1.010	1.163	0.958	0.831	0.15789	0.09	235.17479≈235.17	-4.06
12° 25' S	391.4	118.4	[illegible]	1.009	1.095	0.958	0.882	0.17640	0.10	235.1[illegible]235.19	-4.06

Longitude 33° 26' W
N = 10

Lat.	T_0' (°F)	ΔT	η_T
7° 25' N	235.20	-0.0005	0.10
6° 25' N	235.17	-0.0002	0.09
5° 25' N	235.18	-0.0005	0.08
4° 25' N	235.17	-0.0003	0.07
3° 25' N	235.16	+0.0005	0.06
2° 25' N	235.15	+0.0002	0.05
1° 25' N	235.14	-0.0005	0.04
0° 25' N	235.13	+0.0005	0.03
0° 25' S	235.12	+0.0004	0.02
1° 25' S	235.11	+0.0002	0.01
2° 25' S	235.11	-0.0005	0.01

Longitude 34° 26' W
N = 9

Lat.	T_0' (°F)	ΔT	η_T
7° 25' N	235.19		0.11
6° 25' N	235.17		0.10
5° 25' N	235.18		0.09
4° 25' N	235.17		0.08
3° 25' N	235.16		0.07
2° 25' N	235.15		0.06
1° 25' N	235.14		0.05
0° 25' N	235.13		0.04
0° 25' S	235.12		0.03
1° 25' S	235.12		0.02
2° 25' S	235.11		0.01

Longitude 35° 26' W
N = 8

Lat.	T_0' (°F)	ΔT	η_T
7° 25' N	235.19	+0.0002	0.12
6° 25' N	235.17	-0.0004	0.11
5° 25' N	235.18	+0.0002	0.10
4° 25' N	235.17	+0.0005	0.09
3° 25' N	235.16	+0.0004	0.08
2° 25' N	235.15	+0.0004	0.07
1° 25' N	235.13	+0.0004	0.06
0° 25' N	235.13	-0.0002	0.05
0° 25' S	235.12	+0.0005	0.04
1° 25' S	235.11	-0.0003	0.03
2° 25' S	235.10	-0.0002	0.02

Longitude 36° 26' W
N = 7

Lat.	T_0' (°F)	ΔT	η_T
7° 25' N	235.17	-0.0002	0.10
6° 25' N	235.14	-0.0005	0.09
5° 25' N	235.15	+0.0005	0.08
4° 25' N	235.14	+0.0005	0.07
3° 25' N	235.13	+0.0002	0.06
2° 25' N	235.12	+0.0004	0.05
1° 25' N	235.11	+.0.0005	0.04
0° 25' N	235.10	-0.0002	0.03
0° 25' S	235.09	-0.0005	0.02
1° 25' S	235.08	+0.0003	0.01
2° 25' S	235.08	-0.0005	0.01

Longitude 37° 26' W
N = 6

Lat.	T_0' (°F)	ΔT	η_T
7° 25' N	235.16	-0.0003	0.11
6° 25' N	235.14	+0.0004	0.10
5° 25' N	235.15	-0.0002	0.09
4° 25' N	235.14	-0.0004	0.08
3° 25' N	235.13	+0.0003	0.07
2° 25' N	235.12	-0.0005	0.06
1° 25' N	235.11	+0.0002	0.05
0° 25' N	235.10	+0.0002	0.04
0° 25' S	235.09	+0.0005	0.03
1° 25' S	235.08	+0.0003	0.02
2° 25' S	235.07	-0.0005	0.01

Longitude 38° 26' W
N = 5

Lat.	T_0' (°F)	ΔT	η_T
7° 25' N	235.17	+0.0002	0.12
6° 25' N	235.14	+0.0004	0.11
5° 25' N	235.15	+0.0002	0.10
4° 25' N	235.14	-0.0005	0.09
3° 25' N	235.13	-0.0003	0.08
2° 25' N	235.12	+0.0002	0.07
1° 25' N	235.11	-0.0004	0.06
0° 25' N	235.10	-0.0004	0.05
0° 25' S	235.09	+0.0002	0.04
1° 25' S	235.08	-0.0004	0.03
2° 25' S	235.07	+0.0005	0.02

Longitude 39° 26' W
N = 4

Lat.	T_0' (°F)	ΔT	η_T
7° 25' N	235.14	-0.0005	0.10
6° 25' N	235.11	+0.0003	0.09
5° 25' N	235.12	+0.0005	0.08
4° 25' N	235.11	-0.0002	0.07
3° 25' N	235.10	-0.0005	0.06
2° 25' N	235.09	-0.0003	0.05
1° 25' N	235.08	-0.0005	0.04
0° 25' N	235.07	+0.0004	0.03
0° 25' S	235.06	+0.0005	0.02
1° 25' S	235.05	+0.0005	0.01
2° 25' S	235.05	-0.0003	0.01

Longitude 40° 26' W
N = 3

Lat.	T_0' (°F)	ΔT	η_T
7° 25' N	235.13	-0.0003	0.11
6° 25' N	235.11	-0.0003	0.10
5° 25' N	235.12	+0.0005	0.09
4° 25' N	235.11	-0.0002	0.08
3° 25' N	235.10	-0.0005	0.07
2° 25' N	235.06	+0.0004	0.06
1° 25' N	235.08	+0.0002	0.05
0° 25' N	235.07	+0.0002	0.04
0° 25' S	235.06	+0.0004	0.03
1° 25' S	235.05	-0.0005	0.02
2° 25' S	235.01	+0.0002	0.01

Longitude 41° 26' W
N = 2

Lat.	T_0' (°F)	ΔT	η_T
7° 25' N	235.13	+ 0.0005	0.12
6° 25' N	235.11	+ 0.0005	0.11
5° 25' N	235.12	+ 0.0003	0.10
4° 25' N	235.09	− 0.0005	0.09
3° 25' N	235.10	−0.0002	0.08
2° 25' N	235.11	+0.0004	0.07
1° 25' N	235.08	−0.0005	0.06
0° 25' N	235.07	−0.0002	0.05
0° 25' S	235.06	+0.0002	0.04
1° 25' S	235.05	+0.0004	0.03
2° 25' S	235.06	+0.0002	0.02

Longitude 42° 26' W

Lat.	T_0' (°F)	ΔT	η_T
7° 25' N	235.12	-0.0005 ~~-0.0004~~	0.12
6° 25' N	235.02	-0.0005	0.12
5° 25' N	235.12	+0.0002	0.11
4° 25' N	235.11	-0.0004	0.10
3° 25' N	235.10	-0.0002	0.09
2° 25' N	235.08	+0.0005	0.08
1° 25' N	235.07	+0.0003	0.07
0° 25' N	235.07	+0.0005	0.06
0° 25' S	235.06	-0.0003	0.05
1° 25' S	235.02	+0.0004	0.04
2° 25' S	235.01	-0.0005	0.03

N = 1

Longitude 43° 26' W (SURVEYOR)

Lat	T_0' (°F)	ΔT	η_T
7° 25' N	235.11	+0.0003	0.11
6° 25' N	235.02	-0.0005	0.10
5° 25' N	235.11	+.0.0004	0.09
4° 25' N	235.10	+0.0004	0.08
3° 25' N	235.09	-0.0002	0.07
2° 25' N	235.07	-0.0005	0.06
1° 25' N	235.06	-0.0005	0.05
0° 25' N	235.07	-0.0003	0.04
0° 25' S	235.05	+0.0002	0.03
1° 25' S	235.01	+0.0004	0.02
2° 25' S	235.00	[illegible]	0.01

N = 0

TABLE 3

Predicted Temperatures for Latitudes Greater Than Surveyor's in Area A of Scheme I

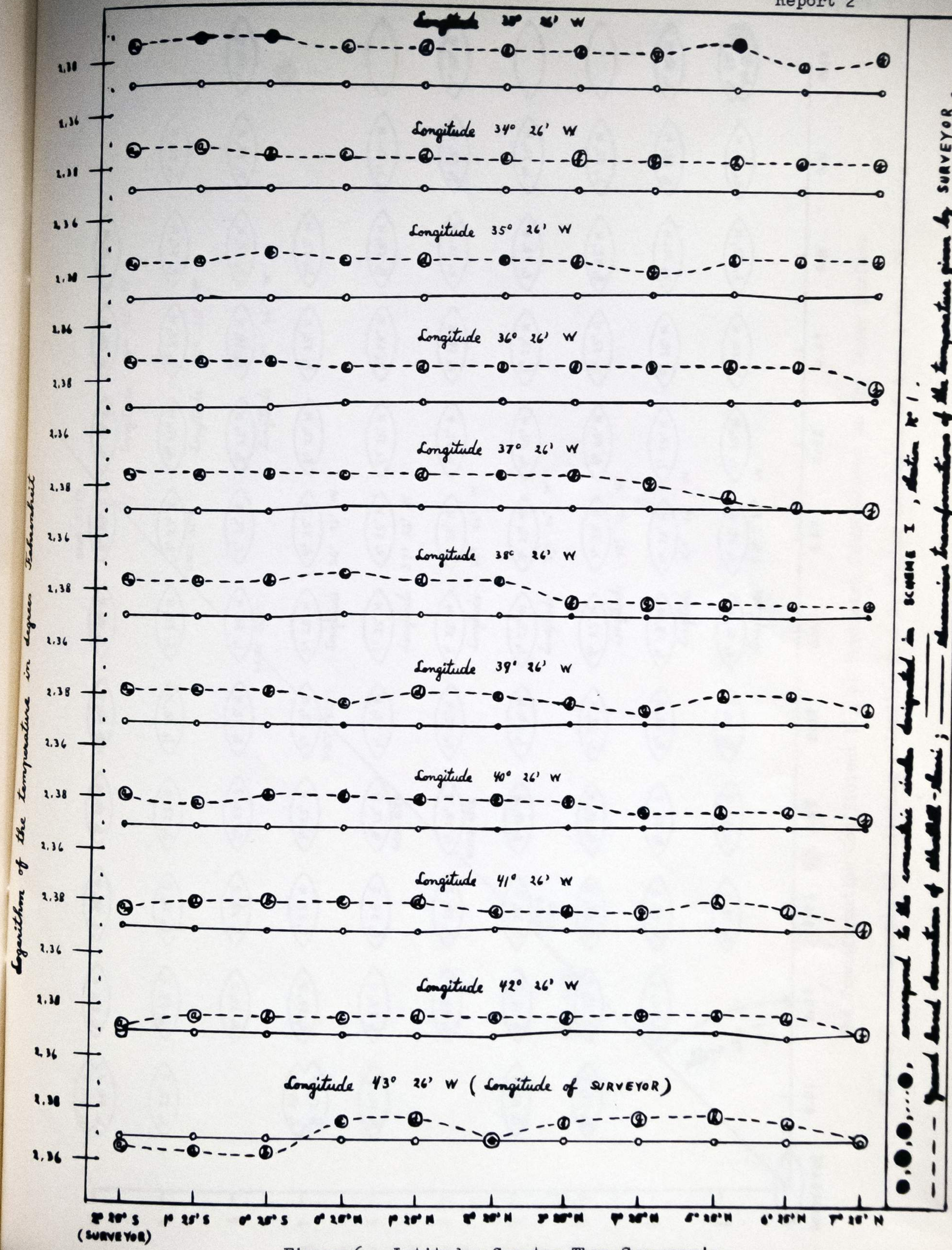

Figure 6. Latitudes Greater Than Surveyor's

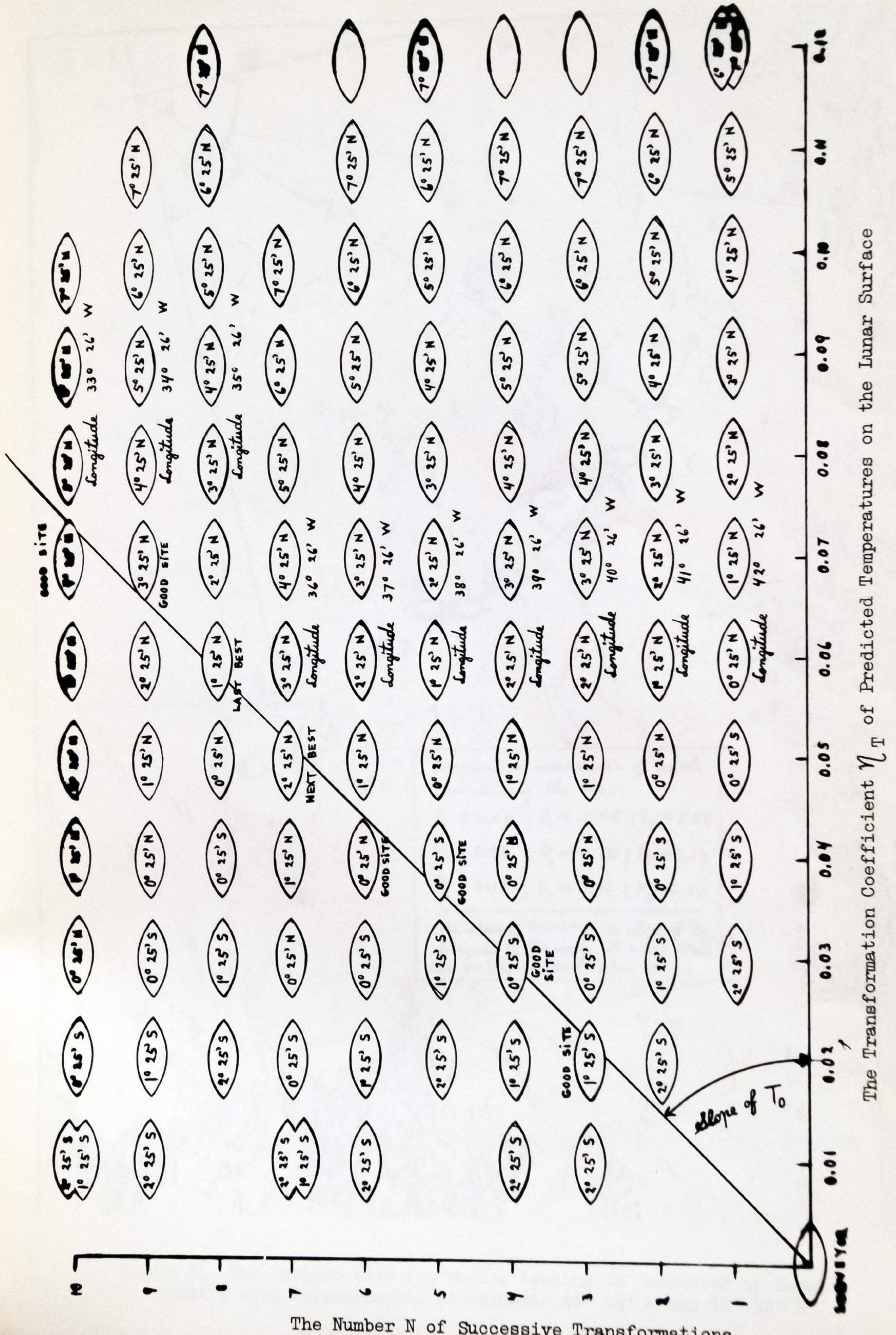

Figure 7. An Example of Selecting a Landing Site in Higher Latitudes of Area A than Surveyor's

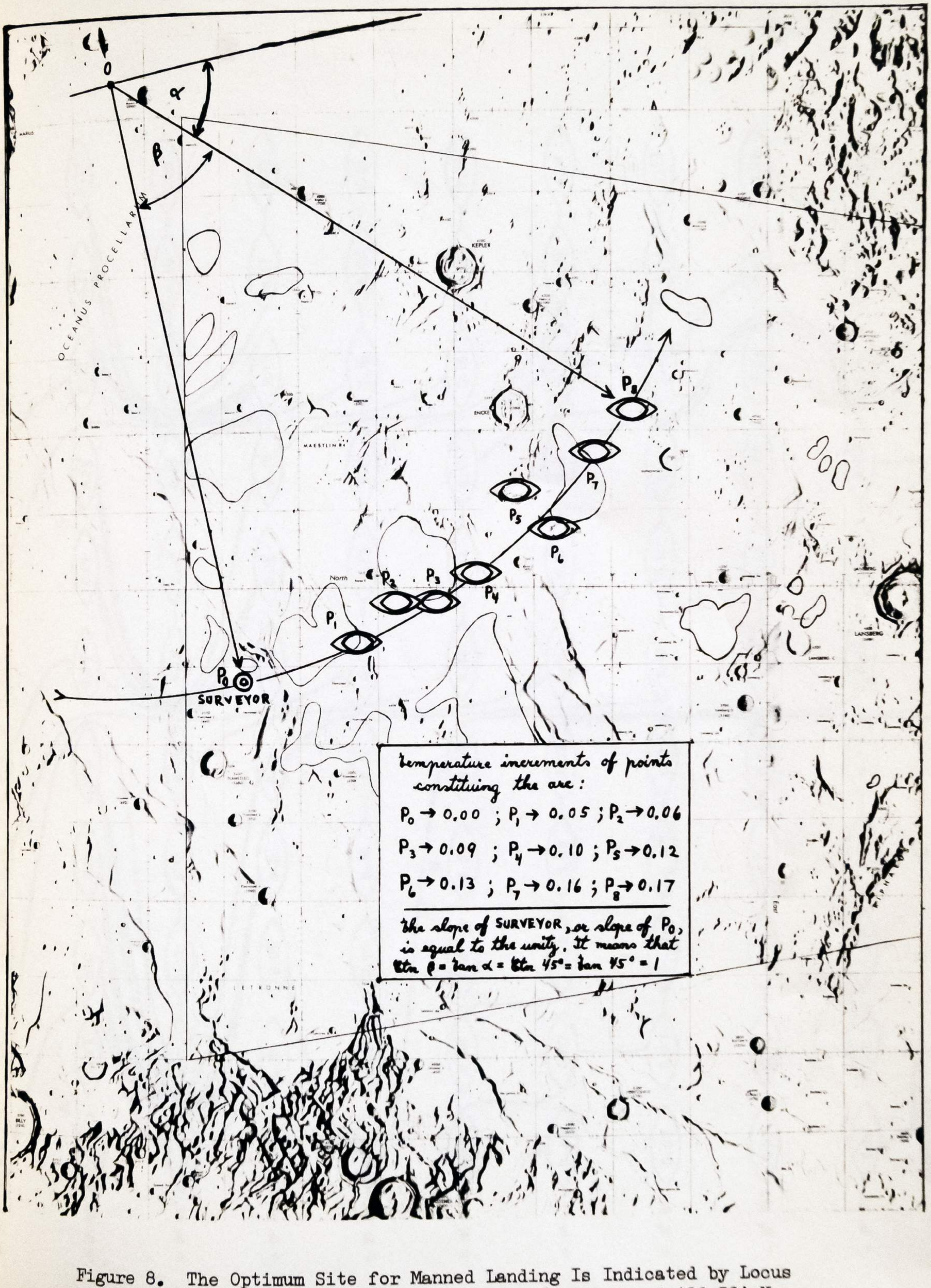

Temperature increments of points constituting the arc:

$P_0 \rightarrow 0.00$; $P_1 \rightarrow 0.05$; $P_2 \rightarrow 0.06$

$P_3 \rightarrow 0.09$; $P_4 \rightarrow 0.10$; $P_5 \rightarrow 0.12$

$P_6 \rightarrow 0.13$; $P_7 \rightarrow 0.16$; $P_8 \rightarrow 0.17$

The slope of SURVEYOR, or slope of P_0, is equal to the unity. It means that $\text{ctn}\ \beta = \tan \alpha = \text{ctn}\ 45° = \tan 45° = 1$

Figure 8. The Optimum Site for Manned Landing Is Indicated by Locus Point O with Selenographic Coordinates 46° 55' W and 12° 52' N

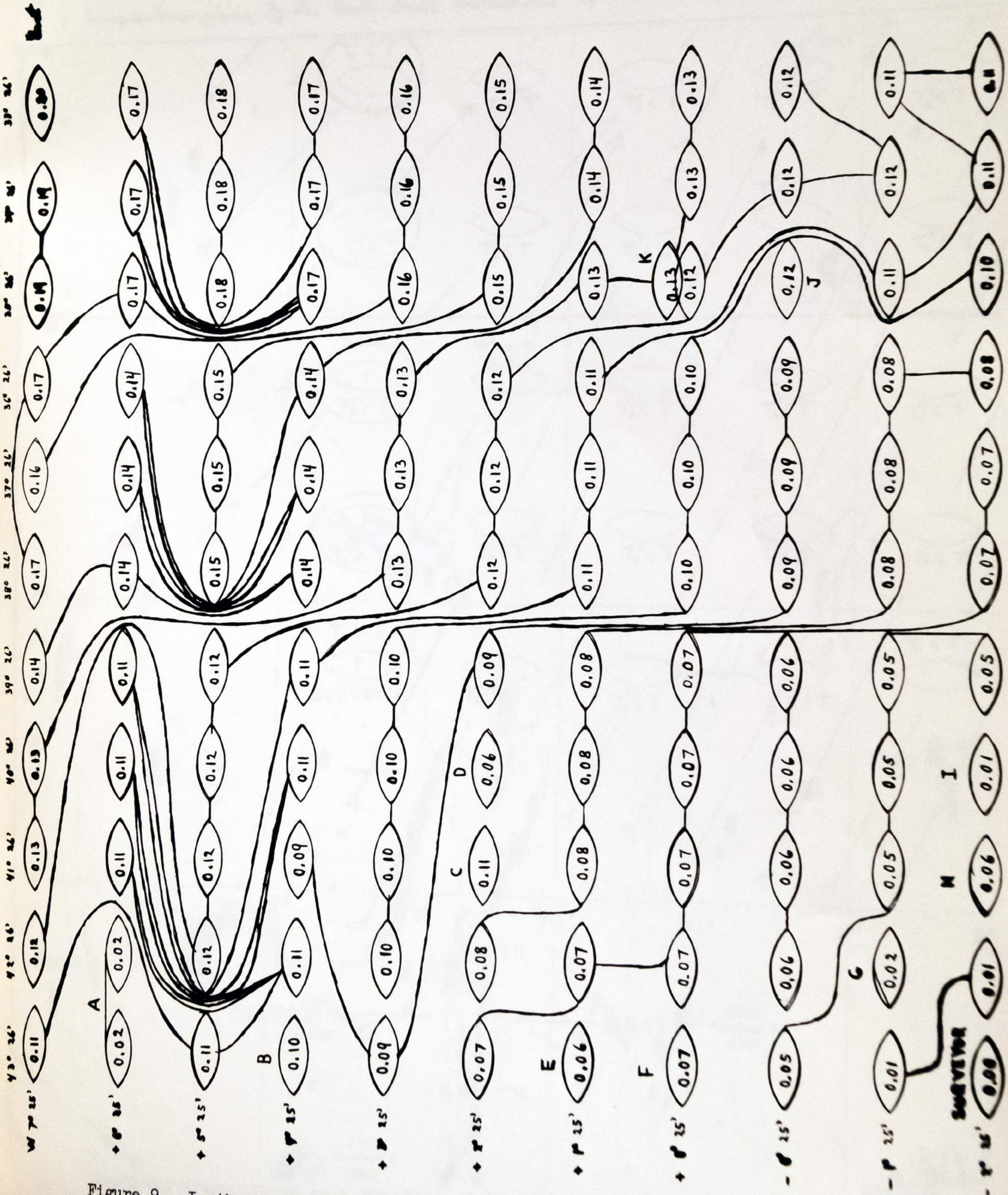

Figure 9. Isotherms for Latitudes Greater Than Surveyor's in Area A of Scheme I

T_0' = Predicted temperatures based on the temperature given by SURVEYOR on the lunar surface.
T = Temperatures given by the Earth-based observations of SHORTHILL-SAARI.

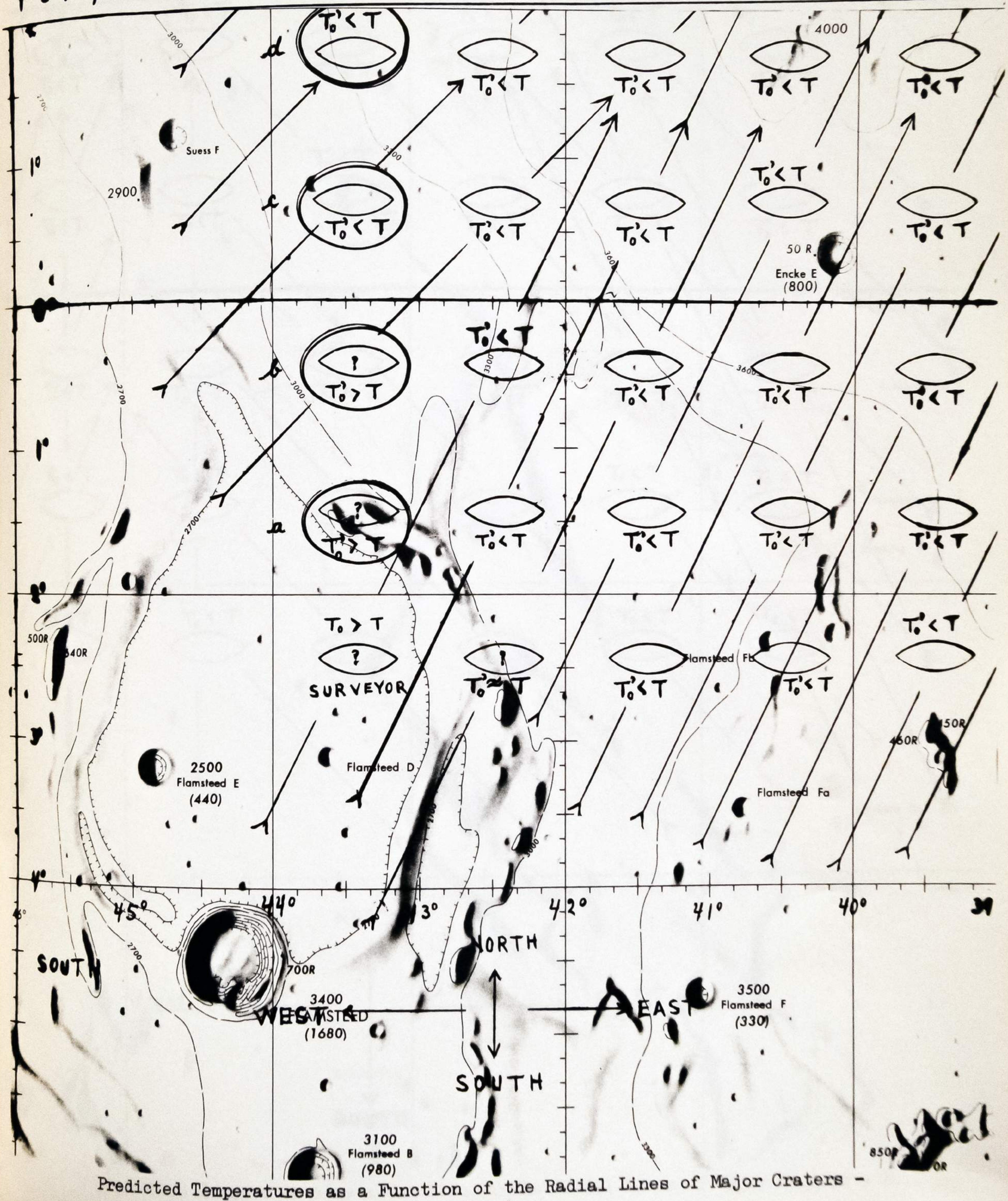

Predicted Temperatures as a Function of the Radial Lines of Major Craters - No. 1

T'_0 = Predicted temperatures based on the temperatures given by SURVEYOR on the lunar surface

T = Temperatures given by the Earth-based observations of SHORTHILL-SAARI.

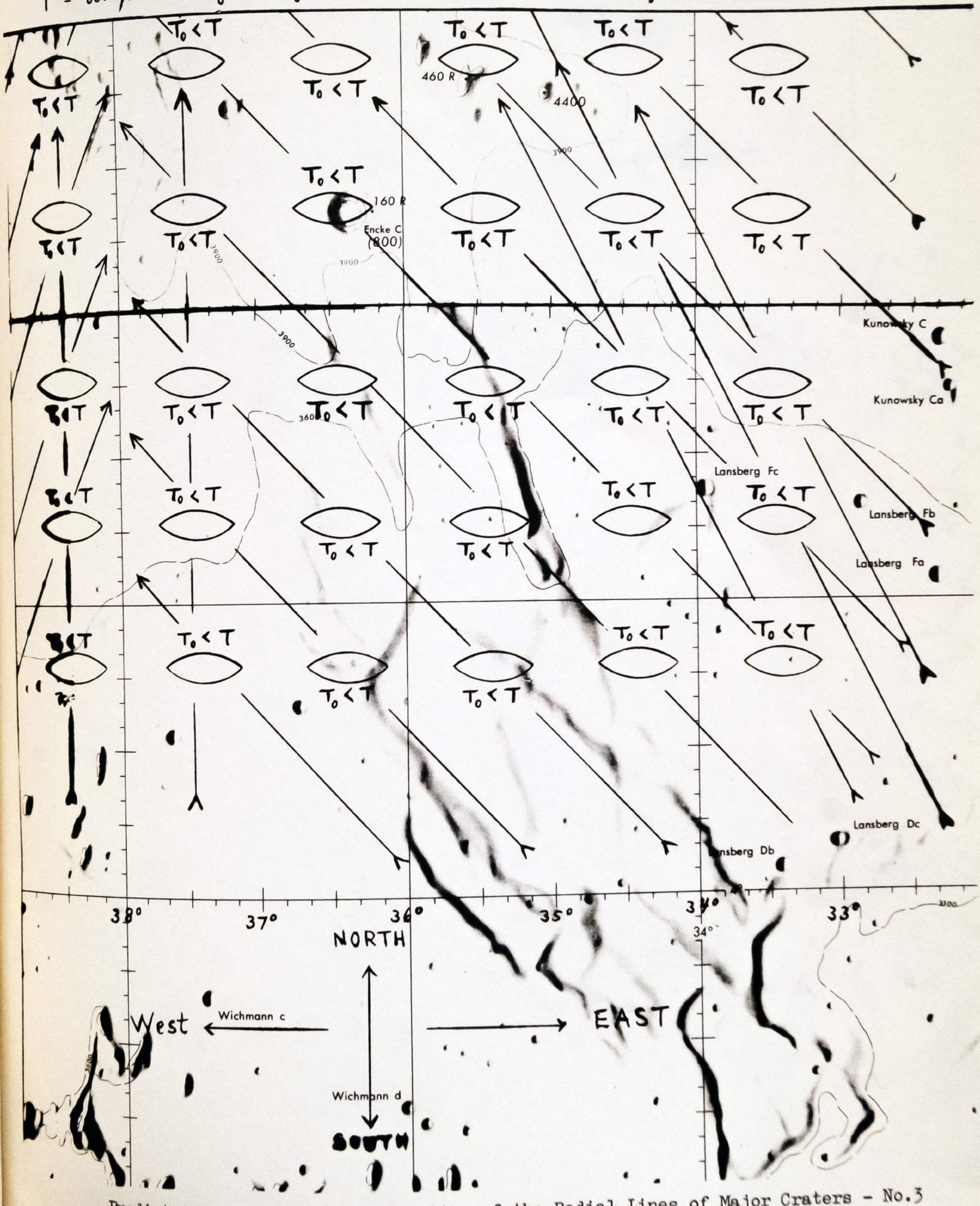

Predicted Temperatures as a Function of the Radial Lines of Major Craters - No.3

T_0' = Predicted temperatures based on the temperatures given by SURVEYOR on the lunar surface.
T = temperatures given by the Earth-based observations of SHORTHILL-SAARI.

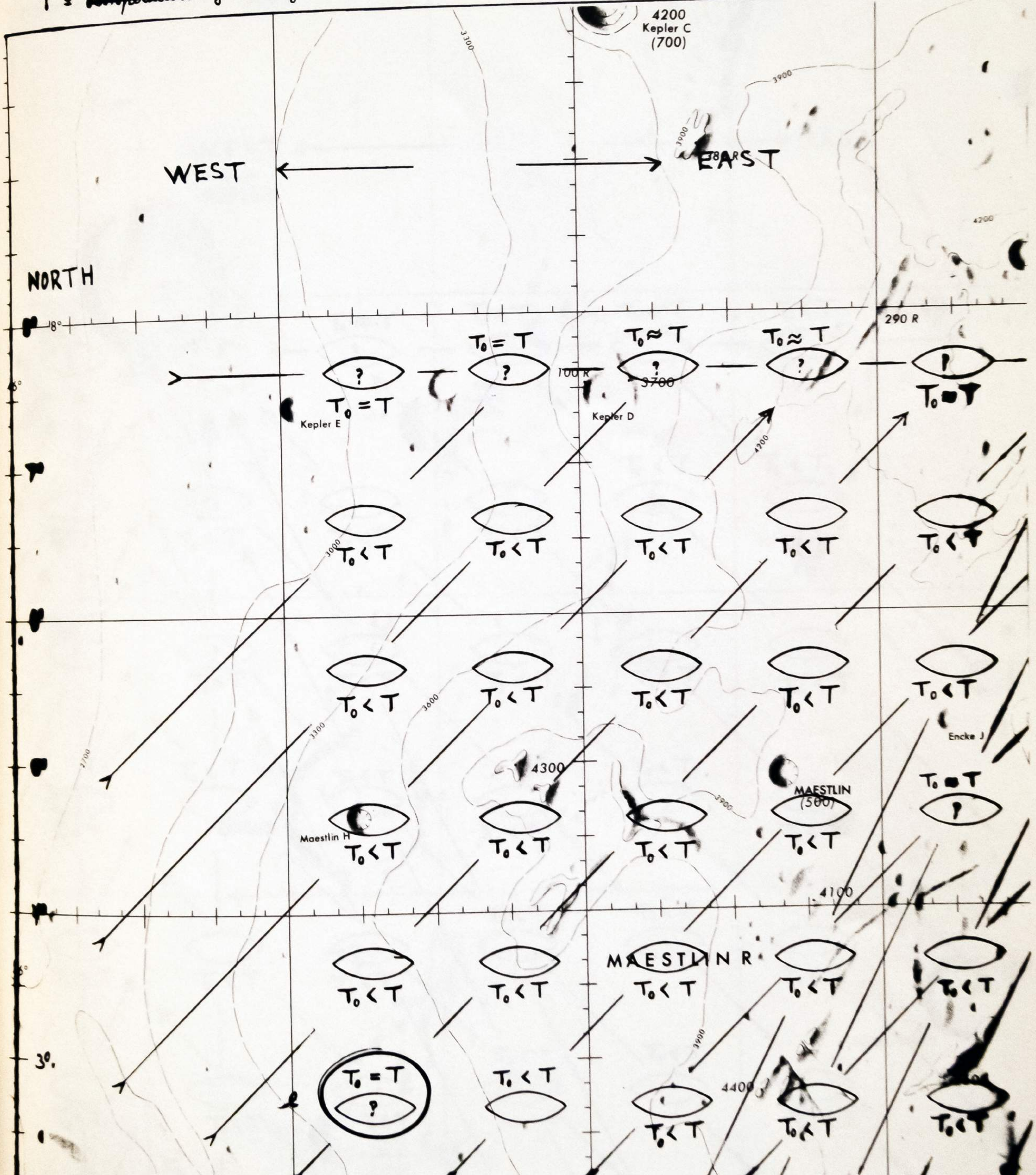

Predicted Temperatures as a Function of the Radial Lines of Major Craters - No.2

T_0' = Predicted temperatures based on the temperatures given by SURVEYOR on the lunar surface.
T = temperatures given by the Earth-based observations of SHORTHILL - SAARI.

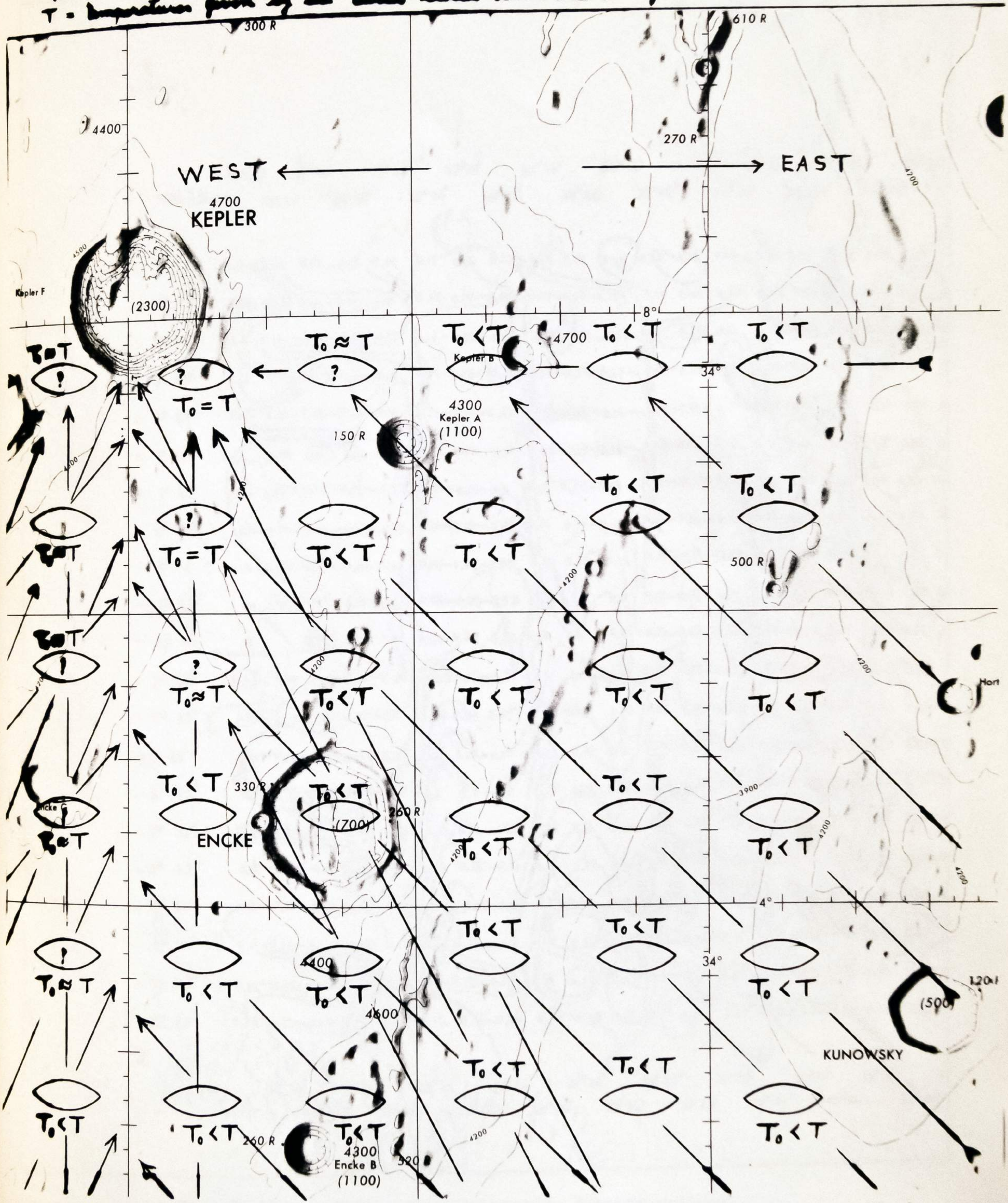

Predicted Temperatures as a Function of the Radial Lines of Major Craters - No.4

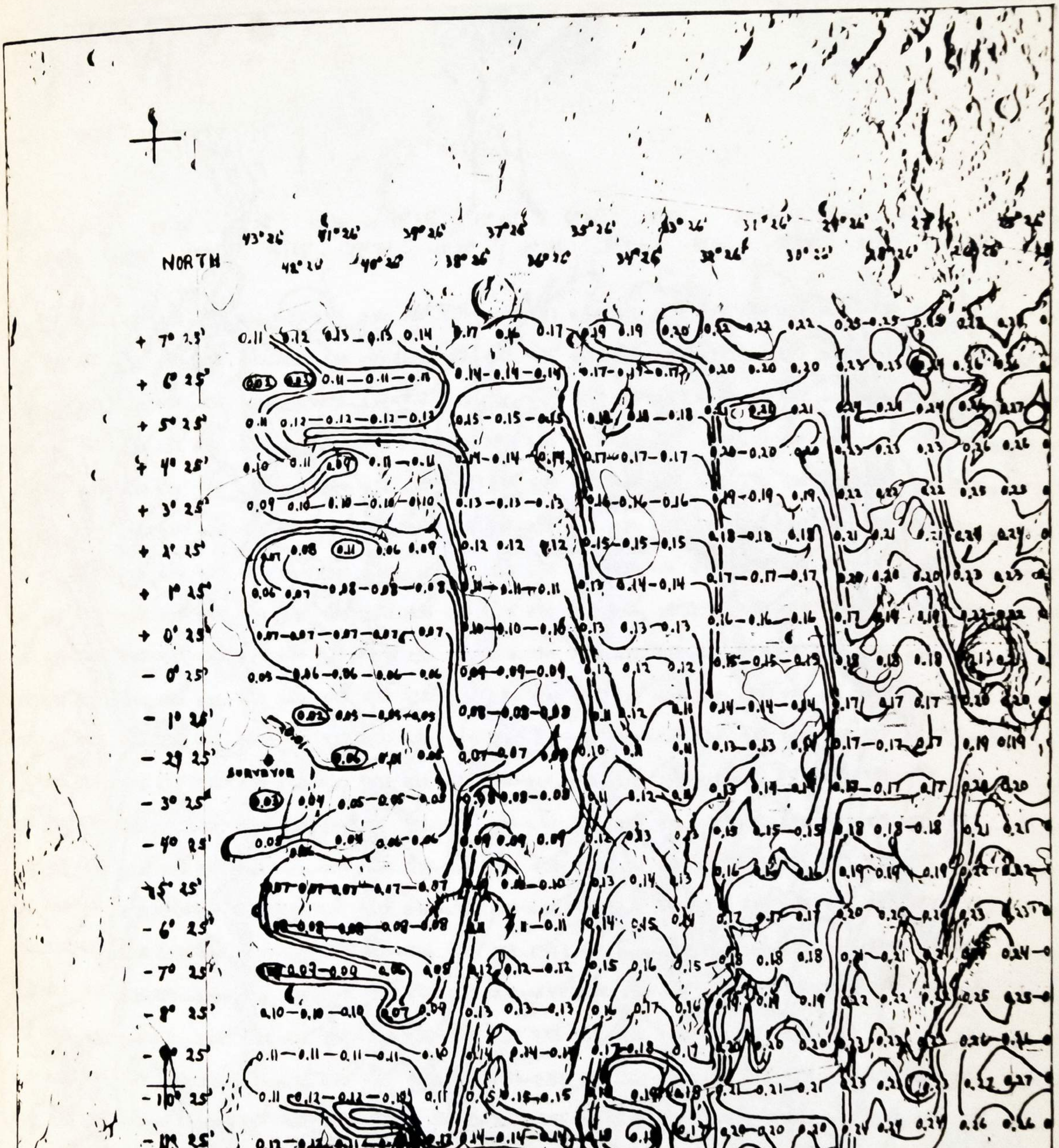

Some Isotherms Obtained by Successive Transformations
for Half of the Apollo Zone - No. 1

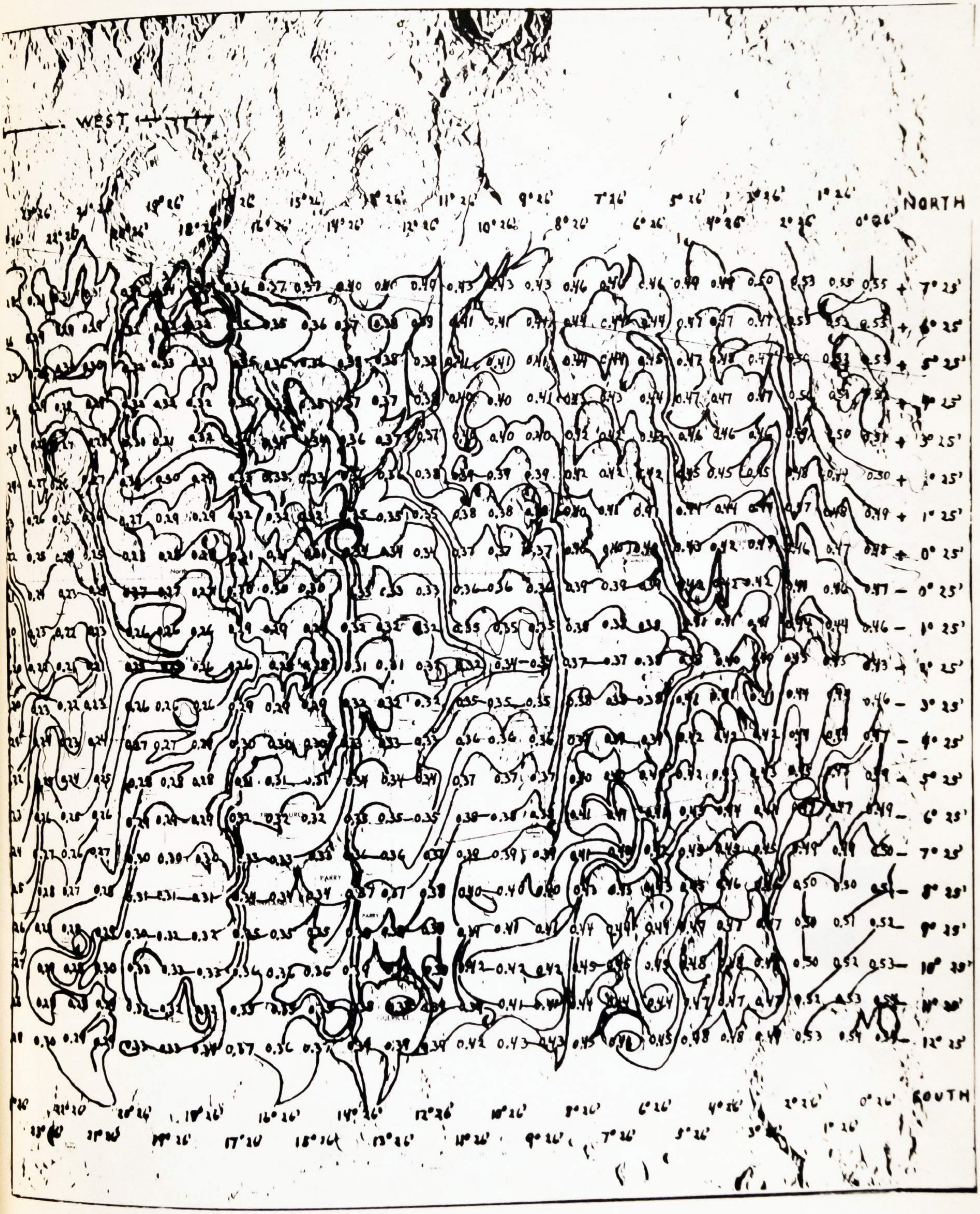

Some Isotherms Obtained by Successive Transformations for Half of the Apollo Zone - No. 2

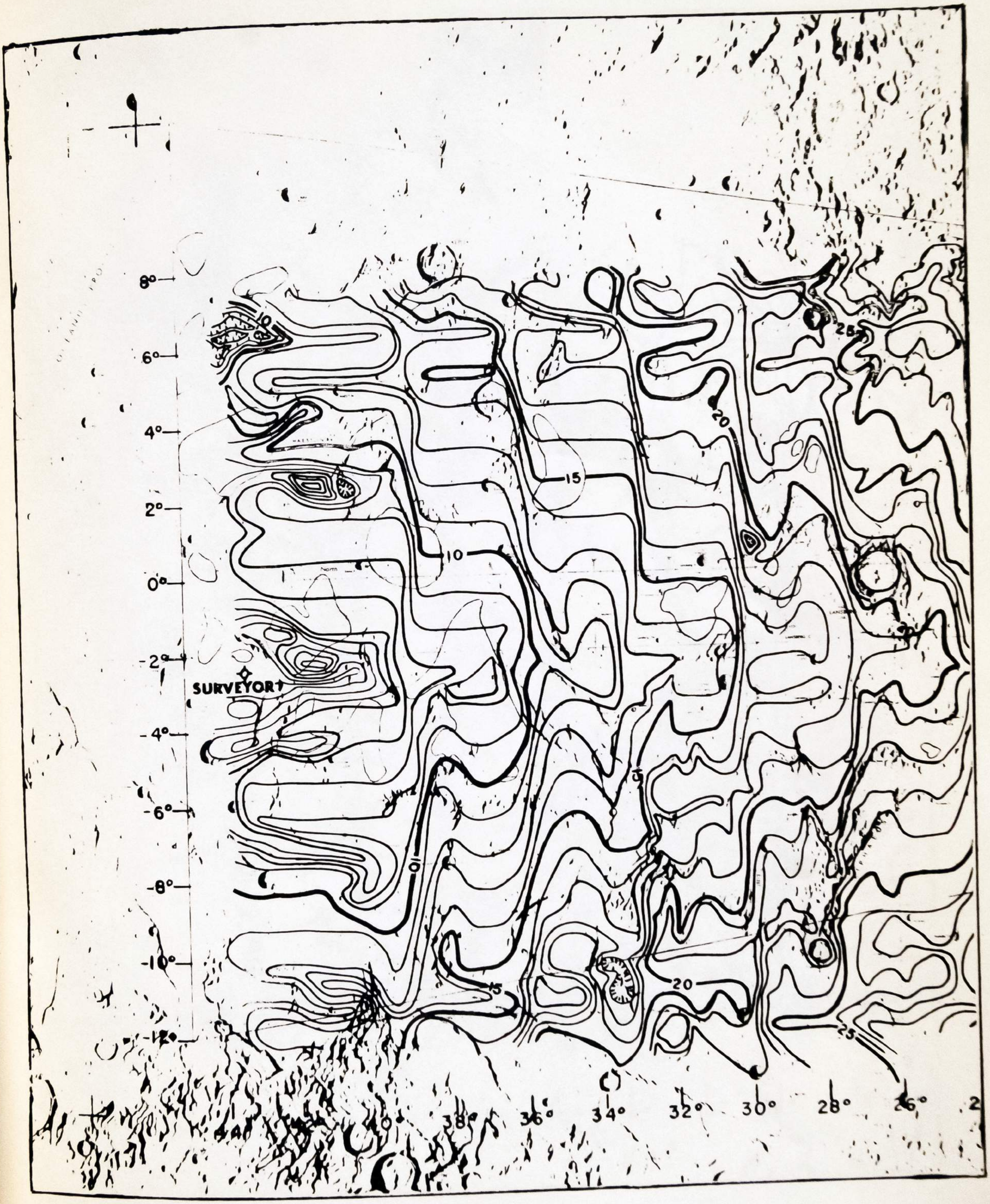

Diagram of the Variation of Multiples - No. 1
(After a Suggestion of Roland R. Vela)

Diagram of the Variation of Multiples - No. 2
(After a Suggestion of Roland R. Vela)